

Correspondence

MIMO Broadcast Channels With Finite-Rate Feedback

Nihar Jindal, *Member, IEEE*

Abstract—Multiple transmit antennas in a downlink channel can provide tremendous capacity (i.e., multiplexing) gains, even when receivers have only single antennas. However, receiver and transmitter channel state information is generally required. In this correspondence, a system where each receiver has perfect channel knowledge, but the transmitter only receives quantized information regarding the channel instantiation is analyzed. The well-known zero-forcing transmission technique is considered, and simple expressions for the throughput degradation due to finite-rate feedback are derived. A key finding is that the feedback rate per mobile must be increased linearly with the signal-to-noise ratio (SNR) (in decibels) in order to achieve the full multiplexing gain. This is in sharp contrast to point-to-point multiple-input multiple-output (MIMO) systems, in which it is not necessary to increase the feedback rate as a function of the SNR.

Index Terms—Broadcast channel, finite rate feedback, multiple-input multiple-output (MIMO) systems, multiplexing gain.

I. INTRODUCTION

In multiple-antenna broadcast (downlink) channels, capacity can be tremendously increased by adding antennas at only the access point (AP) [1], [2]. In essence, an AP equipped with M antennas can support downlink rates up to a factor of M times larger than a single antenna AP, even when each mobile device has only a single antenna.¹ In order to realize these benefits, however, the AP must do the following.

- Simultaneously transmit to multiple users over the same bandwidth (orthogonal schemes such as time-division multiple access (TDMA) or code-division multiple access (CDMA) are generally highly suboptimal).
- Obtain accurate channel state information (CSI).

Practical transmission structures that allow for simultaneous transmission to multiple mobiles, such as downlink beamforming, do exist. The requirement that the AP have accurate CSI, however, is far more difficult to meet, particularly in frequency-division duplexed (FDD) systems. Training can be used to obtain channel knowledge at each of the mobile devices, but obtaining CSI at the AP generally requires feedback from each mobile. Such feedback channels do exist in current systems (e.g., for power control), but the required rate of feedback is clearly an important quantity for system designers.

In this correspondence, we consider the practically motivated finite-rate feedback model, in which each mobile feeds back a finite number of bits regarding its channel instantiation at the beginning of each block. This model was first considered for point-to-point multiple-input multiple-output (MIMO) channels in [3]–[5], where

Manuscript received March 16, 2006; revised July 26, 2006. The material in this correspondence was presented at IEEE Globecom St. Louis, MO November 2005.

The author is with the Department of Electrical and Computer Engineering/Digital Technology Center, University of Minnesota, Minneapolis, MN 55455 USA (e-mail: nihar@umn.edu).

Communicated by P. Viswanath, Associate Editor for Communications.

Color versions of Figs. 2–11 are available online at <http://ieeexplore.ieee.org>. Digital Object Identifier 10.1109/TIT.2006.883550

¹In fact, this is true on the uplink as well, by the multiple-access/broadcast channel duality [2].

the transmitter uses such feedback to more accurately direct its transmitted energy towards the receiver, and even a small number of bits per antenna can be quite beneficial [6]. In point-to-point MIMO channels, the level of CSI available at the transmitter only affects the signal-to-noise ratio (SNR) offset; it does not affect the slope of the capacity versus SNR curve, i.e., the *multiplexing gain*. However, the level of CSI available to the transmitter critically affects the multiplexing gain of the MIMO downlink channel [1]. As a result, channel feedback is considerably more important for MIMO downlink channels than for point-to-point channels.

In contrast to most recent work on the MIMO downlink channel which has primarily concentrated on channels with a very large number of mobiles [7]–[9], we consider systems in which the number of mobiles is equal to the number of transmit antennas. This regime is applicable for inherently smaller systems as well as large systems in which stringent delay constraints do not allow user selection to be performed on the basis of channel qualities, e.g., users are selected for transmission based upon queue lengths instead of on channel conditions. Random beamforming is an alternative limited feedback strategy for MIMO downlink channels in which each mobile feeds back a very low rate quantization of the channel ($\log_2 M$ bits, where M is the number of transmit antennas) as well as an analog SNR value [7]. While this strategy performs well when there are a large number of mobiles relative to the number of transmit antennas, it performs poorly in the small system regime that we consider.

In this work, we propose a simple downlink transmission scheme that uses zero-forcing precoding in conjunction with finite-rate feedback. At the beginning of each block, each mobile quantizes its channel realization to B bits. The AP receives B feedback bits from each mobile and uses zero-forcing precoding based on the channel quantizations. The throughput of such a system is analyzed under the assumption that random quantization codebooks are used by each mobile, i.e., random vector quantization (RVQ) [10], [11] is performed, and that the channel evolves according to an independent and identically distributed (i.i.d.) Rayleigh block-fading model. Our key findings are as follows:

- The throughput of a feedback-based zero-forcing system is bounded if the SNR is taken to infinity and the number of feedback bits per mobile is kept fixed.
- The number of feedback bits per mobile (B) must be increased *linearly* with the SNR (in decibels) at the rate

$$B = (M - 1) \log_2 P \\ \approx \frac{M - 1}{3} P_{dB}$$

in order to achieve the full multiplexing gain of M . In addition, this scaling of B guarantees that the throughput loss relative to perfect CSIT-based zero-forcing is upper-bounded by M bits per second per hertz (bps/Hz), which corresponds to a 3-dB power offset.

- Scaling the number of feedback bits according to $B = \alpha \log_2 P$ for any $\alpha < M - 1$ results in a strictly inferior multiplexing gain of $M \left(\frac{\alpha}{M-1} \right)$.

In essence, the channel estimation error at the AP must scale as the inverse of the SNR in order to achieve the full multiplexing gain if the proposed zero-forcing-based architecture is used, which results in the

required linear scaling of feedback. As a result of this scaling, the required feedback load is quite high in systems operating at even moderate SNR levels. However, it may be feasible to support such loads if the feedback channels experience the same SNR as the downlink channel and high-rate transmission is used for feedback. While the above conclusions are initially derived for RVQ, it is also shown that the fundamental results on the bounded throughput of a fixed feedback-rate system and on the required scaling of feedback rate in proportion to SNR are not limited to RVQ-based systems but also apply to *any* quantization codebook design.

The MIMO downlink finite-rate feedback model was also considered independently by Ding, Love, and Zoltowski [12], and MIMO downlink channels with unquantized (analog) feedback are studied by Samardzija and Mandayam in [13].

The remainder of this correspondence is organized as follows. In Section II, we describe the channel model and the finite-rate feedback mechanism. In Section III, we provide background material on MIMO downlink capacity, linear precoding, and random vector quantization. In Section IV, we describe the proposed zero-forcing-based system, and analyze the throughput of this system (assuming RVQ is used) in Section V. Section VI extends a number of results to arbitrary quantization schemes. We provide numerical results comparing finite-rate feedback systems to alternative transmission techniques in Section VII, and close by discussing conclusions and possible extensions of this work in Section VIII.

II. SYSTEM MODEL

We consider a K receiver multiple-antenna broadcast channel in which the transmitter (also referred to as the AP) has $M > 1$ antennas and each receiver has a single antenna. The broadcast channel is mathematically described as

$$y_i = \mathbf{h}_i^\dagger \mathbf{x} + n_i, \quad i = 1, \dots, K \quad (1)$$

where $\mathbf{h}_1, \mathbf{h}_2, \dots, \mathbf{h}_K$ are the channel vectors (with $\mathbf{h}_i \in \mathbb{C}^{M \times 1}$) of users 1 through K , the vector $\mathbf{x} \in \mathbb{C}^{M \times 1}$ is the transmitted signal, and n_1, \dots, n_K are independent complex Gaussian noise terms with unit variance. The input must satisfy a transmit power constraint of P , i.e., $E[\|\mathbf{x}\|^2] \leq P$. We denote the concatenation of the channels by $\mathbf{H}^\dagger = [\mathbf{h}_1^\dagger \mathbf{h}_2^\dagger \dots \mathbf{h}_K^\dagger]$, i.e., \mathbf{H} is $K \times M$ with the i th row equal to the channel of the i th receiver (\mathbf{h}_i^\dagger). In order to focus our efforts on the impact of imperfect CSI, we consider a system where the number of mobiles is equal to the number of transmit antennas, i.e., $K = M$.

The channel is assumed to be block fading, with independent fading from block to block. The entries of the channel vectors are distributed as i.i.d. unit variance complex Gaussians (Rayleigh fading). Furthermore, each of the receivers is assumed to have perfect and instantaneous knowledge of its own channel vector, i.e., \mathbf{h}_i . Notice it is not required for mobiles to know the channel of other mobiles. Partial CSI is acquired at the transmitter via a finite rate feedback channel from each of the mobiles, as described below.

In the finite-rate feedback model shown in Fig. 1 each receiver quantizes its channel to B bits and feeds back the bits perfectly and instantaneously to the AP, which is assumed to have no other knowledge of the instantaneous state of the channel. The quantization is performed using a vector quantization codebook that is known at the transmitter and the receivers. Typically, each mobile uses a different codebook to prevent multiple mobiles from quantizing their channel to the same quantization vector. A quantization codebook \mathcal{C} consists of 2^B M -dimensional unit norm vectors $\mathcal{C} \triangleq \{\mathbf{w}_1, \dots, \mathbf{w}_{2^B}\}$, where B is the number of feedback bits per mobile. Similar to point-to-point MIMO systems, each

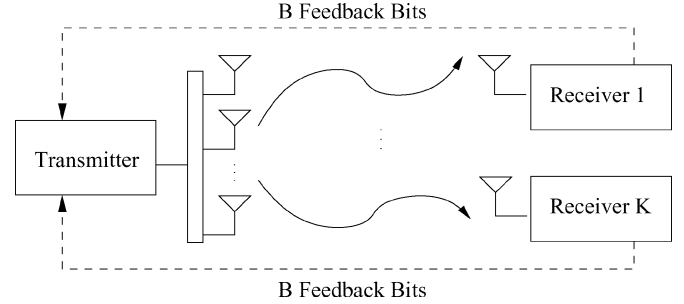


Fig. 1. Finite-rate feedback system model.

receiver quantizes its channel to the quantization vector that is closest to its channel vector, where closeness is measured in terms of the angle between two vectors or, equivalently, the inner product [4], [5]. Thus, user i computes quantization index F_i according to

$$\begin{aligned} F_i &= \arg \max_{j=1, \dots, 2^B} |\mathbf{h}_i^\dagger \mathbf{w}_j| \\ &= \arg \min_{j=1, \dots, 2^B} \sin^2(\angle(\mathbf{h}_i, \mathbf{w}_j)) \end{aligned} \quad (2)$$

and feeds this index back to the transmitter. Note that only the direction of the channel vector is quantized, and no information regarding the channel magnitude is conveyed to the transmitter. Magnitude information can be used to perform power and rate loading across multiple channels, but this is generally of secondary concern when the number of mobiles is the same as the number of antennas.²

Clearly, the choice of vector quantization codebook significantly affects the quality of the CSI provided to the AP. In this work, we primarily focus on performance assuming RVQ, in which an ensemble of quantization codebooks is considered. Details of RVQ are discussed in Section III-C.

Notation

We use boldface to denote vectors and matrices and \mathbf{A}^\dagger refers to the conjugate transpose, or Hermitian, of \mathbf{A} . The notation $\|\mathbf{x}\|$ refers the Euclidean norm of the vector \mathbf{x} , and $\angle(\mathbf{x}, \mathbf{y})$ refers to the angle between vectors \mathbf{x} and \mathbf{y} with the standard convention

$$|\cos(\angle(\mathbf{x}, \mathbf{y}))| = |\mathbf{x}^\dagger \mathbf{y}| / (\|\mathbf{x}\| \cdot \|\mathbf{y}\|).$$

III. BACKGROUND

A. Capacity Results for MIMO Broadcast Channels

In this section, we summarize relevant capacity results for the multiple-antenna broadcast channel. When perfect CSI is available at transmitter and receivers, the capacity region of the channel is achieved by dirty-paper coding [15], [1], [16]–[18], which is a technique that can be used to pre-cancel multiuser interference at the transmitter [19]. In this correspondence, we study the total system throughput, or the sum rate, which we denote as $C_{\text{sum}}^{\text{sum}}(\mathbf{H}, P)$. At high SNR, the sum rate capacity of the MIMO broadcast channel (BC) can be approximated as [20]

$$C_{\text{TX}/\text{RX}-\text{CSI}}^{\text{sum}}(\mathbf{H}, P) \approx M \log(P) + c \quad (3)$$

where c is a constant depending on the channel realization \mathbf{H} . The key feature to notice is that capacity grows *linearly* as a function of

²If there are more users than antennas (i.e., $K > M$) and user selection is allowed, channel magnitude information can provide a significant benefit to the user selection process [14].

M . Though the K (total) receive antennas are distributed among K receivers, the linear growth is the same as in an M -transmit, K -receive antenna point-to-point MIMO system, i.e., both systems have the same *multiplexing gain*.

If each of the mobiles suffers from fading according to the same distribution and the transmitter has no instantaneous CSI, the situation is very different. In this scenario, the channels of all receivers are statistically identical, and thus the channel is degraded, in any order. Therefore, any codeword receiver 1 can decode can also be decoded by any other receiver, which implies that a TDMA strategy is optimal [21, Sec. VI], [22]. Thus, the sum capacity of this channel is equal to the capacity of the point-to-point channel from the transmitter to any individual receiver

$$C_{\text{RX-CSI}}^{\text{sum}} = E_{\mathbf{h}_1} \left[\log \left(1 + \frac{P}{M} \|\mathbf{h}_1\|^2 \right) \right] \quad (4)$$

and, therefore, the multiplexing gain of this channel is only one. In fact, the downlink channel achieves a multiplexing gain of only one for any fading distribution in which the spatial direction of each channel is isotropically distributed, independent of the channel norm [22]. This includes a channel in which users have unequal average SNRs but each suffers from spatially uncorrelated Rayleigh fading.

There clearly is a huge gap between the capacity of the MIMO downlink channel with transmitter CSI (multiplexing gain of M) and without transmitter CSI (multiplexing gain of 1). Thus, it is of interest to investigate the more practical assumption of partial CSI at the AP. If each of the mobiles has perfect CSI and the AP has imperfect CSI of fixed quality (e.g., Rician fading with a fixed variance that is independent of the SNR), it has recently been shown that the multiplexing gain of the sum capacity is strictly smaller than M [23].³ Somewhat complementary to this result, our work shows that the full multiplexing gain of M can be achieved if the feedback rate (i.e., the quality of the CSI) is increased as a function of SNR such that the estimation error goes to zero as the inverse of SNR.

B. Linear Precoding

Though dirty-paper coding is capacity achieving for the MIMO broadcast channel, the technique requires considerable complexity and practical implementations are still being actively pursued [24]–[26]. As a result, simpler downlink transmission schemes are of obvious interest. One such scheme is linear precoding, which is also referred to as downlink beamforming, which incurs a rate/power loss relative to dirty-paper coding but achieves the same multiplexing gain of M . While there are certainly many other powerful MIMO downlink transmission techniques, such as the nonlinear precoding technique proposed in [27], linear precoding has been shown to perform extremely well in comparison to such schemes [28].

In order to implement this scheme, the transmitter multiplies the symbol intended for each receiver by a beamforming vector and transmits the sum of these vector signals. Let s_i denote the scalar symbol intended for the i th receiver, and let \mathbf{v}_i denote the corresponding unit norm beamforming vector. The transmitted signal is then given by $\mathbf{x} = \sum_{j=1}^K \mathbf{v}_j s_j$. The received signal at user i is therefore,

$$y_i = \mathbf{h}_i^\dagger \mathbf{x} + n_i = \sum_{j=1}^K \mathbf{h}_i^\dagger \mathbf{v}_j s_j + n_i \quad (5)$$

and the SINR at mobile i is

$$\text{SINR}_i = \frac{\frac{P}{M} |\mathbf{h}_i^\dagger \mathbf{v}_i|^2}{1 + \sum_{j \neq i} \frac{P}{M} |\mathbf{h}_i^\dagger \mathbf{v}_j|^2} \quad (6)$$

³It is conjectured that the multiplexing gain in this scenario is in fact equal to one, although this has yet to be shown.

under the assumption that each of the symbols has power P/M . If the inputs s_1, \dots, s_K are chosen i.i.d. complex Gaussian, rates up to $I(S_i; Y_i | \mathbf{H}) = \log_2(1 + \text{SINR}_i)$ are achievable with standard single-user detection (i.e., no interference cancellation is attempted). Note that the capacity-achieving strategy is linear precoding with the addition of a precoding step at the transmitter which leads to the elimination of some of the multiuser interference terms in the signal-to-interference-plus-noise ratio (SINR) expression.

The performance of linear precoding clearly depends on the choice of beamforming vectors, but the problem of determining the sum rate maximizing beamforming vectors is generally very difficult. One simple choice of beamforming vectors are the zero-forcing vectors, which are chosen such that no multiuser interference is experienced at any of the receivers. This can be done by choosing the beamforming vector of user i orthogonal to the channel vectors of all other users, i.e., by choosing \mathbf{v}_i orthogonal to \mathbf{h}_j for all $i \neq j$. It is easily seen that the zero-forcing beamforming vectors are simply the normalized columns of the inverse of the concatenated channel matrix \mathbf{H} . If such beamforming vectors are used, the received signal at the i th mobile reduces to

$$y_i = \mathbf{h}_i^\dagger \mathbf{x} + n_i = \sum_{j=1}^K \mathbf{h}_i^\dagger \mathbf{v}_j s_j + n_i = \mathbf{h}_i^\dagger \mathbf{v}_i s_i + n_i \quad (7)$$

because $\mathbf{h}_i^\dagger \mathbf{v}_j = 0$ for all $j \neq i$ by construction. Since all interference has been eliminated, the corresponding SNR is given as $\text{SNR}_i = \frac{P}{M} |\mathbf{h}_i^\dagger \mathbf{v}_i|^2$. In fact, zero-forcing is optimal among all downlink beamforming strategies at asymptotically optimal at high SNR [20].

Since zero-forcing creates M independent and parallel channels, the resulting multiplexing gain is equal to M , which is the same as for the capacity-achieving DPC strategy. Zero-forcing does however, incur a rate loss (or alternatively, a power loss) relative to capacity. At high SNR, the power loss of zero forcing relative to dirty-paper coding converges to

$$\frac{3 \log_2 e}{M} \sum_{j=1}^{M-1} \frac{j}{M-j} \text{ decibels}$$

which is approximately equal to $3 \log_2 M$ decibels [20]. Clearly, the transmitter must have perfect channel knowledge in order to choose the zero-forcing beamforming vectors. If there is any imperfection in this knowledge, there inevitably will be some multiuser interference, which leads to performance degradation.

C. Random Vector Quantization

In this work, we use RVQ, in which each of the 2^B quantization vectors is independently chosen from the isotropic distribution on the M -dimensional unit sphere [10], [11]. We analyze performance averaged over all such choices of random codebooks, in addition to averaging over the fading distribution. Random codebooks are used because the optimal vector quantizer for this problem is not known in general, and known bounds are rather loose. RVQ, on the other hand, is very amenable to analysis and also performs measurably close to optimal quantization, as is shown in Section VI. Similar to the standard random coding argument used for channel coding, there always exists at least one quantization codebook that performs at least as well as the ensemble average. Note that each receiver is assumed to use a different and independently generated quantization codebook; if a common codebook were used, there would be a nonzero probability that multiple users return the same quantization vector, which reduces the number of spatial dimensions available.

RVQ was first used to analyze the performance of CDMA and point-to-point MIMO channels with finite-rate feedback, and has been shown to be asymptotically optimal in the large system limit

(e.g., infinitely many antennas) [10], [11]. There has also been very recent work characterizing the error performance of point-to-point multiple-input, single-output (MISO) systems utilizing RVQ [29].

We now review some basic results on RVQ from [29] that will be useful in later derivations. As stated earlier, the quantization vectors are i.i.d. isotropic vectors on the M -dimensional unit sphere, as are the channel directions $\tilde{\mathbf{h}}_i \triangleq \frac{\mathbf{h}_i}{\|\mathbf{h}_i\|}$ due to the assumption of i.i.d. Rayleigh fading. The most important quantity of interest is the statistical distribution of the quantization error. In order to determine this, first consider the inner product between a channel direction and an arbitrary quantization vector

$$\left| \mathbf{w}_j^\dagger \tilde{\mathbf{h}}_i \right|^2 = \cos^2 \left(\angle(\tilde{\mathbf{h}}_i, \mathbf{w}_j) \right).$$

Because $\tilde{\mathbf{h}}_i$ and \mathbf{w}_j are independent isotropic vectors, the quantity

$$\left| \mathbf{w}_j^\dagger \tilde{\mathbf{h}}_i \right|^2 = \cos^2 \left(\angle(\tilde{\mathbf{h}}_i, \mathbf{w}_j) \right)$$

is beta distributed with parameters 1 and $M - 1$, and

$$\sin^2 \left(\angle(\tilde{\mathbf{h}}_i, \mathbf{w}_j) \right) = 1 - \cos^2 \left(\angle(\tilde{\mathbf{h}}_i, \mathbf{w}_j) \right)$$

is beta distributed with parameters $M - 1$ and 1. Thus, the cumulative distribution function (cdf) of $X = \sin^2 \left(\angle(\tilde{\mathbf{h}}_i, \mathbf{w}_j) \right)$ is given by $\Pr(X \leq x) = x^{M-1}$.

Let $\hat{\mathbf{h}}_i$ denote the quantization of the vector \mathbf{h}_i , i.e., the solution to (2). Since the quantization vectors are independent, the quantization error $Z \triangleq \sin^2 \left(\angle(\tilde{\mathbf{h}}_i, \hat{\mathbf{h}}_i) \right)$ is the minimum of 2^B independent beta $(M - 1, 1)$ random variables, and the complementary cdf (ccdf) of Z is given by $\Pr(Z \geq z) = (1 - z^{M-1})^{2^B}$ [29, Lemma 1]. The expectation of this quantity has been computed in closed form [29]

$$E_{\mathbf{H}, \mathcal{W}} \left[\sin^2 \left(\angle(\tilde{\mathbf{h}}_i, \hat{\mathbf{h}}_i) \right) \right] = 2^B \cdot \beta \left(2^B, \frac{M}{M-1} \right). \quad (8)$$

Here we use $\beta(\cdot)$ to denote the beta function, which is defined in terms of the gamma function as $\beta(x, y) = \frac{\Gamma(x)\Gamma(y)}{\Gamma(x+y)}$ [30]. The gamma function is the extension of the factorial function to non-integers, and satisfies the fundamental properties $\Gamma(n) = (n-1)!$ for positive integers and $\Gamma(x+1) = x\Gamma(x)$ for all x [30]. While the derivation of (8) given in [29] depends on the Pochmann symbol, this result can alternatively be derived using an integral representation of the beta function, as shown in Appendix I. Furthermore, a simple extension of inequalities given in [29] gives a strict upper bound to the expected quantization error.

Lemma 1: The expected quantization error can be upper-bounded as

$$E_{\mathbf{H}, \mathcal{W}} \left[\sin^2 \left(\angle(\tilde{\mathbf{h}}_i, \hat{\mathbf{h}}_i) \right) \right] < 2^{-\frac{B}{M-1}}.$$

Proof: See Appendix II. \square

To gain some intuition, consider that the “ideal” Voronoi region around a quantization vector is a (two-sided) spherical cap of area 2^{-B} , and $\sin^2(\cdot)$ of the angle between the center and a vector on the boundary of such a cap is equal to $2^{-\frac{B}{M-1}}$. Numerical results indicate that this bound is tight in the difference sense but not in the ratio sense as $B \rightarrow \infty$. However, it is not difficult to show (using Lemma 6 and (21) from Section VI) that the above quantity is lower-bounded by $(\frac{M-1}{M})2^{-\frac{B}{M-1}}$ and therefore is quite accurate in the even ratio sense. Our later results indicate that the bound is indeed sufficiently precise to accurately characterize throughput degradation due to finite-rate feedback.

D. Point-to-Point MISO Systems With Finite Rate Feedback

In this section, we briefly review some basic results on point-to-point MISO systems (i.e., M transmit antennas, single receive antenna, which is equivalent to the given system model with $K = 1$) with finite-rate feedback, under the assumption of i.i.d. Rayleigh fading. If the transmitter has perfect CSI, it is well known that the optimum transmission strategy is to beamform along the channel vector \mathbf{h} [31] and the corresponding (ergodic) capacity is

$$C_{\text{CSIT}}(P) = E_{\mathbf{h}} \left[\log \left(1 + P \|\mathbf{h}\|^2 \right) \right].$$

If the transmitter has no channel state information transmitter (CSIT) and only has knowledge of the fading distribution, the optimum transmission strategy is to transmit independent and equal power signals from each of the M transmit antennas, and the corresponding capacity is

$$C_{\text{no-CSIT}}(P) = E_{\mathbf{h}} \left[\log \left(1 + \frac{P}{M} \|\mathbf{h}\|^2 \right) \right].$$

Clearly

$$C_{\text{no-CSIT}}(P) = C_{\text{CSIT}} \left(\frac{P}{M} \right)$$

and therefore, the lack of CSIT leads to a $10 \log_{10} M$ -decibel SNR loss relative to perfect CSIT.

Providing the transmitter with partial CSIT via a finite-rate feedback channel can be used to reduce this SNR loss. If the transmitter acquires CSIT through the finite-rate feedback channel, an optimal or nearly optimal strategy is to beamform in the direction of the quantization vector.⁴ The average rate achieved with this strategy assuming RVQ is used is given by

$$\begin{aligned} R_{\text{FB}}(P) &= E_{\mathbf{h}, \mathcal{W}} \left[\log \left(1 + P \|\mathbf{h}\|^2 \cos^2 \left(\angle(\mathbf{h}, \hat{\mathbf{h}}) \right) \right) \right] \\ &\approx E_{\mathbf{h}} \left[\log \left(1 + P \|\mathbf{h}\|^2 (1 - 2^{-\frac{B}{M-1}}) \right) \right] \end{aligned}$$

where we have based the approximation on the upper bound given in Lemma 1, which is numerically quite accurate. Thus, the use of limited feedback leads to an SNR degradation of approximately $10 \log_{10} (1 - 2^{-\frac{B}{M-1}})$ decibels relative to perfect CSIT. Note that this approximation agrees with the expression derived for an asymptotically large number of transmit antennas in [11]. If $B = M - 1$, for example, a finite-rate feedback system is expected to perform within about 3 dB of a perfect CSIT system. The capacity with CSIT, no CSIT, and finite-rate feedback with $B = M - 1 = 3$ is shown for a 4×1 MISO system in Fig. 2. Notice that there is a 6-dB gap between the CSIT and no CSIT curves, while the finite-rate feedback curve is 2.7 dB from the perfect CSIT curve, which is quite close to our approximation of 3 dB.

The key point is that the feedback load need not be increased as a function of SNR in order to maintain a constant power or rate gap relative to the perfect CSIT capacity curve in point-to-point MISO channels. This is perhaps not surprising, since the amount of feedback only affects the $\cos^2 \left(\angle(\mathbf{h}, \hat{\mathbf{h}}) \right)$ term and thus leads to only an SNR degradation. Furthermore, also note that the multiplexing gain (i.e., the slope of the capacity curve) is not affected by the level of CSIT. For the MIMO downlink channel, however, the multiplexing gain of an M -transmit antenna, K user system is $\min(N, K)$ when there is perfect CSIT, but is only 1 if there is no CSIT. Clearly, such a channel will be considerably more sensitive to the accuracy of the CSIT obtained through the finite-rate feedback channels.

⁴Conditions for the optimality of beamforming along the quantization direction are provided in [32]. Though these conditions are difficult to analytically compute for most quantization codebooks, it is generally well accepted that beamforming performs extremely close to capacity.

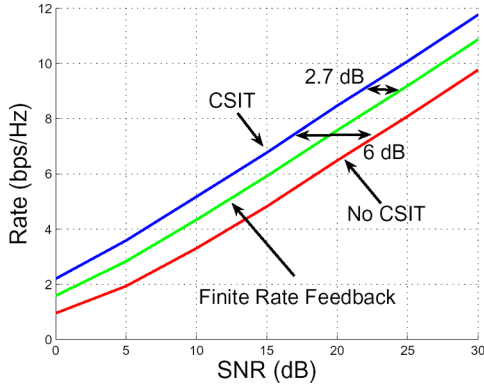


Fig. 2. 4×1 MISO system with CSIT, no CSIT, and feedback.

IV. ZERO-FORCING PRECODING WITH FINITE-RATE FEEDBACK

In this section, we describe the proposed zero-forcing-based transmission scheme. After the transmitter has received feedback bits from each of the K receivers, an appropriate multiuser transmission strategy must be chosen. We propose using *zero-forcing beamforming* based on the channel quantizations available at the transmitter. Zero-forcing is a low-complexity transmission scheme that can be implemented by a simple linear precoder, and its performance is optimal among the set of all linear precoders at asymptotically high SNR [20]. We later provide numerical results describing the performance of *regularized* zero-forcing precoding [27], which outperforms pure zero-forcing at low SNRs but is equivalent to zero-forcing at asymptotically high SNR.

Note that dirty-paper coding cannot be directly applied in this scenario because of the imperfection in CSIT. In order to implement dirty-paper coding, the transmitter requires knowledge of the multiuser interference at the receiver, and not at the transmitter. The received interference clearly depends on the channel state, which is not known perfectly at the transmitter in the finite-rate feedback model. The transmitter could estimate the received interference based on the available channel quantization, but even this estimated interference cannot be canceled perfectly using dirty-paper coding due to the transmitter's imperfect knowledge of the received signal power. In order to implement dirty-paper coding, the transmitter must also know the received SNR (in the absence of any interference) in order to properly select the *inflation factor*, which is a key component in the dirty-paper coding implementation [24]. Since the SNR also depends on the channel realization, the transmitter only has an imperfect estimate of the SNR and thus cannot properly select the inflation factor.

When the transmitter has perfect CSI, zero-forcing can be used to completely eliminate multiuser interference by precoding transmission by the inverse of the channel matrix \mathbf{H} . This creates a parallel, noninterfering channel to each of the M receivers, and thus leads to a multiplexing gain of M . In the finite-rate feedback setting, the imperfection in CSIT makes it impossible to completely eliminate all multiuser interference, but a zero-forcing-based strategy can still be quite effective. Since the transmitter only has knowledge of the channel quantizations but does not have any information regarding the magnitude or spatial direction of the quantization error, a reasonable approach to take is to select beamforming vectors according to the zero-forcing criterion based on the channel quantizations.

Let $\hat{\mathbf{h}}_i$ refer to the quantized version of mobile i 's channel. These quantized vectors are compiled into a matrix

$$\hat{\mathbf{H}} = [\hat{\mathbf{h}}_1 \quad \hat{\mathbf{h}}_2 \quad \cdots \quad \hat{\mathbf{h}}_M]^\dagger.$$

The matrix $\hat{\mathbf{H}}$ is the estimate of the channels, upon which zero-forcing is performed. Thus, the beamforming vectors are chosen to be the normalized columns of the matrix $\hat{\mathbf{H}}^{-1}$. If equal power $\frac{P}{M}$ is used for each of the data streams, the received SINR at the i th mobile is given by (6):

$$\text{SINR}_i = \frac{\frac{P}{M} |\hat{\mathbf{h}}_i^\dagger \mathbf{v}_i|^2}{1 + \sum_{j \neq i} \frac{P}{M} |\hat{\mathbf{h}}_i^\dagger \mathbf{v}_j|^2}. \quad (9)$$

Since the beamforming vectors are chosen orthogonal to the channel quantizations and not the actual channel realizations, the interference terms in the denominator of the SINR expression are not zero. However, these terms directly depend on the quantization error and thus can be analyzed using the statistics of random vector quantization.

We study long-term average throughput (over both the fading distribution and RVQ), and thus rate $R_i = E_{\mathbf{H}, \mathcal{W}} [\log_2(1 + \text{SINR}_i)]$ can be achieved to user i if Gaussian inputs are used. By symmetry, the system throughput is given by

$$R_{\text{FB}}(P) \triangleq M E_{\mathbf{H}, \mathcal{W}} [\log_2(1 + \text{SINR}_1)].$$

For a system that achieves a throughput of $R(P)$ (where P is the SNR, or power constraint), the multiplexing gain is defined as

$$r = \lim_{P \rightarrow \infty} \frac{R(P)}{\log_2(P)}. \quad (10)$$

V. THROUGHPUT ANALYSIS

In this section, we analyze the throughput of a feedback-based zero-forcing system utilizing random vector quantization. We first state some useful preliminary calculations, and then study the achieved throughput for fixed and increasing feedback levels.

A. Preliminary Calculations

In this subsection, we prove a few useful results regarding the distribution of terms in the SINR expression in (9). For the remainder of this correspondence, we use $\hat{\mathbf{h}}_i$ to denote the normalized channel vector, i.e., $\hat{\mathbf{h}}_i = \mathbf{h}_i / \|\mathbf{h}_i\|$. Using this notation, we can rewrite the SINR as

$$\text{SINR}_i = \frac{\frac{P}{M} \|\hat{\mathbf{h}}_i\|^2 |\hat{\mathbf{h}}_i^\dagger \mathbf{v}_i|^2}{1 + \sum_{j \neq i} \frac{P}{M} \|\hat{\mathbf{h}}_j\|^2 |\hat{\mathbf{h}}_i^\dagger \mathbf{v}_j|^2}. \quad (11)$$

We first make a simple observation regarding the numerator of this expression.

Observation 1: The beamforming vector \mathbf{v}_i is isotropically distributed in \mathbb{C}^M and is independent of the channel direction $\hat{\mathbf{h}}_i$ as well as the channel quantization $\hat{\mathbf{h}}_i$.

By the zero-forcing procedure, \mathbf{v}_i is chosen in the nullspace of $\{\hat{\mathbf{h}}_j\}_{j \neq i}$. Since RVQ is used and the channel directions $\{\hat{\mathbf{h}}_j\}_{j \neq i}$ are independent isotropic vectors, the channel quantizations $\hat{\mathbf{h}}_1, \dots, \hat{\mathbf{h}}_M$ are mutually independent isotropically distributed vectors. Thus, the nullspace of $\{\hat{\mathbf{h}}_j\}_{j \neq i}$ is an isotropically distributed direction in \mathbb{C}^M , independent of either $\hat{\mathbf{h}}_i$ or $\hat{\mathbf{h}}_i$. Clearly, the same is true if the transmitter performs zero-forcing on the basis of perfect CSIT (i.e., $\hat{\mathbf{h}}_i = \hat{\mathbf{h}}_i$).

Next we characterize the interference terms that appear in the denominator of the SINR expression:

Lemma 2: The random variable $|\hat{\mathbf{h}}_i^\dagger \mathbf{v}_j|^2$ for any $i \neq j$ is equal to the product of the quantization error $\sin^2(\angle(\hat{\mathbf{h}}_i, \hat{\mathbf{h}}_i))$ and an independent beta $(1, M - 2)$ random variable.

Proof: Without loss of generality, consider $i = 2$ and $j = 1$, i.e., the term $|\hat{\mathbf{h}}_2^\dagger \mathbf{v}_1|^2$. The vector \mathbf{v}_1 is chosen in the nullspace of $\hat{\mathbf{h}}_2, \dots, \hat{\mathbf{h}}_M$, each of which is an independent isotropically distributed vector. Therefore, \mathbf{v}_1 is isotropically distributed within the $(M - 1)$ -dimensional nullspace of $\hat{\mathbf{h}}_2$. Now consider the normalized channel vector $\tilde{\mathbf{h}}_2$. Since RVQ is used, the quantization error has no preferential direction, i.e., the error is isotropically distributed in \mathbb{C}^M . Thus, conditioned on the magnitude of the quantization error $a \triangleq \sin^2(\angle(\tilde{\mathbf{h}}_2, \hat{\mathbf{h}}_2))$, the channel direction can be written as the sum of two vectors, one in the direction of the quantization, and the other isotropically distributed in the nullspace of the quantization: $\tilde{\mathbf{h}}_2 = \sqrt{1-a}\hat{\mathbf{h}}_2 + \sqrt{a}\mathbf{s}$, where \mathbf{s} is a unit norm vector isotropically distributed in the nullspace of $\hat{\mathbf{h}}_2$, and is independent of a . Therefore, the random variable $\tilde{\mathbf{h}}_2$ can be written as

$$\tilde{\mathbf{h}}_2 = (\sqrt{1-Z})\hat{\mathbf{h}}_2 + \sqrt{Z}\mathbf{s}$$

where \mathbf{s} and Z are independent, with \mathbf{s} isotropically distributed in the nullspace of $\hat{\mathbf{h}}_2$ and Z distributed according to the quantization error distribution, i.e., the minimum of 2^B beta $(M - 1, 1)$ random variables, as described in Section III-C.

The inner product of $\tilde{\mathbf{h}}_2$ and \mathbf{v}_1 is then given by

$$\begin{aligned} |\tilde{\mathbf{h}}_2^\dagger \mathbf{v}_1|^2 &= (1-Z)|\hat{\mathbf{h}}_2^\dagger \mathbf{v}_1|^2 + Z|\mathbf{s}^\dagger \mathbf{v}_1|^2 \\ &= Z|\mathbf{s}^\dagger \mathbf{v}_1|^2. \end{aligned}$$

Since \mathbf{s} and \mathbf{v}_1 are i.i.d. isotropic vectors in the $(M - 1)$ -dimensional nullspace of $\hat{\mathbf{h}}_2$, the quantity $|\mathbf{s}^\dagger \mathbf{v}_1|^2$ is beta $(1, M - 2)$ distributed, and is independent of Z . \square

Since a beta random variable has support $[0, 1]$, we have

$$|\tilde{\mathbf{h}}_i^\dagger \mathbf{v}_j|^2 \leq \sin^2(\angle(\tilde{\mathbf{h}}_i, \hat{\mathbf{h}}_i)), \quad \forall i \neq j \quad (12)$$

i.e., the interference from any single user is no larger than the quantization error. When $M = 2$, we clearly have $|\tilde{\mathbf{h}}_i^\dagger \mathbf{v}_j|^2 = \sin^2(\angle(\tilde{\mathbf{h}}_i, \hat{\mathbf{h}}_i))$, and no beta random variable is needed.

Finally, a derivation of the expectation of the logarithm of the quantization error, which is useful in a few subsequent theorems, is given as follows.

Lemma 3: The expectation of the logarithm of the quantization error is given by

$$E_{\mathbf{H}, \mathbf{W}} \left[\log_2 \left(\sin^2(\angle(\tilde{\mathbf{h}}_i, \hat{\mathbf{h}}_i)) \right) \right] = -\frac{\log_2 e}{M-1} \sum_{k=1}^{2^B} \frac{1}{k}.$$

Furthermore, this quantity can be bounded as

$$\frac{B}{M-1} \leq -E_{\mathbf{H}, \mathbf{W}} \left[\log_2 \left(\sin^2(\angle(\tilde{\mathbf{h}}_i, \hat{\mathbf{h}}_i)) \right) \right] \leq \frac{B + \log_2 e}{M-1}.$$

Proof: See Appendix III. \square

B. Fixed-Feedback Quality

We now analyze the average throughput achieved by the proposed zero-forcing scheme, and quantify the performance degradation as a function of the feedback rate. In order to study the performance loss, we define the rate gap $\Delta R(P)$ to be the difference between the per mobile throughput achieved by perfect CSIT-based zero-forcing and finite-rate feedback-based zero-forcing

$$\Delta R(P) \triangleq \frac{1}{M} [R_{ZF}(P) - R_{FB}(P)].$$

In this expression $R_{ZF}(P)$ refers to the throughput achieved by perfect CSIT-based zero-forcing (i.e., $\tilde{\mathbf{h}}_i = \hat{\mathbf{h}}_i$), which is given by

$$R_{ZF}(P) = ME_{\mathbf{H}} \left[\log_2 \left(1 + \frac{P}{M} |\mathbf{h}_i^\dagger \mathbf{v}_{ZF,i}|^2 \right) \right]$$

where each beamforming vector $\mathbf{v}_{ZF,i}$ is chosen orthogonal to $\{\mathbf{h}_j\}_{j \neq i}$.

Theorem 1: Finite-rate feedback with B feedback bits per mobile incurs a throughput loss relative to perfect CSIT zero-forcing upper-bounded by

$$\Delta R(P) < \log_2 \left(1 + P \cdot 2^{-\frac{B}{M-1}} \right).$$

Proof: The rate gap can be upper-bounded as

$$\begin{aligned} \Delta R(P) &= E_{\mathbf{H}} \left[\log_2 \left(1 + \frac{P}{M} |\mathbf{h}_i^\dagger \mathbf{v}_{ZF,i}|^2 \right) \right] - \\ &E_{\mathbf{H}, \mathbf{W}} \left[\log_2 \left(1 + \frac{\frac{P}{M} |\mathbf{h}_i^\dagger \mathbf{v}_i|^2}{1 + \sum_{j \neq i} \frac{P}{M} |\mathbf{h}_i^\dagger \mathbf{v}_j|^2} \right) \right] \\ &= E_{\mathbf{H}} \left[\log_2 \left(1 + \frac{P}{M} |\mathbf{h}_i^\dagger \mathbf{v}_{ZF,i}|^2 \right) \right] - \\ &E_{\mathbf{H}, \mathbf{W}} \left[\log_2 \left(1 + \frac{P}{M} |\mathbf{h}_i^\dagger \mathbf{v}_i|^2 + \sum_{j \neq i} \frac{P}{M} |\mathbf{h}_i^\dagger \mathbf{v}_j|^2 \right) \right] \\ &+ E_{\mathbf{H}, \mathbf{W}} \left[\log_2 \left(1 + \sum_{j \neq i} \frac{P}{M} |\mathbf{h}_i^\dagger \mathbf{v}_j|^2 \right) \right] \\ &\stackrel{(a)}{\leq} E_{\mathbf{H}} \left[\log_2 \left(1 + \frac{P}{M} |\mathbf{h}_i^\dagger \mathbf{v}_{ZF,i}|^2 \right) \right] - \\ &E_{\mathbf{H}, \mathbf{W}} \left[\log_2 \left(1 + \frac{P}{M} |\mathbf{h}_i^\dagger \mathbf{v}_i|^2 \right) \right] \\ &+ E_{\mathbf{H}, \mathbf{W}} \left[\log_2 \left(1 + \sum_{j \neq i} \frac{P}{M} |\mathbf{h}_i^\dagger \mathbf{v}_j|^2 \right) \right] \\ &\stackrel{(b)}{=} E_{\mathbf{H}, \mathbf{W}} \left[\log_2 \left(1 + \sum_{j \neq i} \frac{P}{M} |\mathbf{h}_i^\dagger \mathbf{v}_j|^2 \right) \right] \end{aligned}$$

where (a) follows because $\sum_{j \neq i} \frac{P}{M} |\mathbf{h}_i^\dagger \mathbf{v}_j|^2 \geq 0$ and $\log(\cdot)$ is a monotonically increasing function. To get (b), note that $\mathbf{v}_{ZF,i}$ and \mathbf{v}_i are each isotropically distributed unit vectors, independent of \mathbf{h}_i (Observation 1), which implies

$$E_{\mathbf{H}} \left[\log_2 \left(1 + \frac{P}{M} |\mathbf{h}_i^\dagger \mathbf{v}_{ZF,i}|^2 \right) \right] = E_{\mathbf{H}, \mathbf{W}} \left[\log_2 \left(1 + \frac{P}{M} |\mathbf{h}_i^\dagger \mathbf{v}_i|^2 \right) \right]$$

Applying Jensen's inequality to the upper bound in (b) and exploiting the independence of the channel norm (which satisfies $E[\|\mathbf{h}_i\|^2] = M$) and channel direction, we get

$$\begin{aligned} \Delta R(P) &\leq \log_2 \left(1 + \frac{P}{M} (M-1) E[\|\mathbf{h}_i\|^2] E[|\tilde{\mathbf{h}}_i^\dagger \mathbf{v}_j|^2] \right) \\ &= \log_2 \left(1 + P(M-1) E[|\tilde{\mathbf{h}}_i^\dagger \mathbf{v}_j|^2] \right). \end{aligned}$$

By Lemma 2, the term $E[|\tilde{\mathbf{h}}_i^\dagger \mathbf{v}_j|^2]$ is the product of the expectation of the quantization error and the expectation of a beta $(1, M - 2)$ random variable, which is equal to $\frac{1}{M-1}$. Using Lemma 1, we have

$$\begin{aligned} \Delta R(P) &\leq \log_2 \left(1 + P \cdot E[\sin^2(\angle(\tilde{\mathbf{h}}_i, \hat{\mathbf{h}}_i))] \right) \\ &< \log_2 \left(1 + P \cdot 2^{-\frac{B}{M-1}} \right). \quad \square \end{aligned}$$

The most important feature to notice is that the rate loss is an increasing function of the system SNR (P) , which can be explained by

the linear relationship between P and the multiuser interference power. This intuition motivates the following result, which shows that a finite-rate feedback system with fixed feedback quality is interference-limited at high SNR.

Theorem 2: The throughput achieved by finite-rate feedback-based zero-forcing with a fixed number of feedback bits per mobile B is bounded as the SNR is taken to infinity

$$R_{\text{FB}}(P) \leq M \left(1 + \frac{B + \log_2 e}{M-1} + \log_2(M-2) + \log_2 e \right).$$

Proof: Consider the following upper bounds to the throughput $R_{\text{FB}}(P)$:

$$\begin{aligned} \frac{1}{M} R_{\text{FB}}(P) &= E_{\mathbf{H}, \mathcal{W}} \left[\log_2 \left(1 + \frac{\frac{P}{M} \|\mathbf{h}_i\|^2 |\tilde{\mathbf{h}}_i^\dagger \mathbf{v}_i|^2}{1 + \sum_{j \neq i} \frac{P}{M} \|\mathbf{h}_i\|^2 |\tilde{\mathbf{h}}_i^\dagger \mathbf{v}_j|^2} \right) \right] \\ &\stackrel{(a)}{\leq} E_{\mathbf{H}, \mathcal{W}} \left[\log_2 \left(1 + \frac{|\tilde{\mathbf{h}}_i^\dagger \mathbf{v}_i|^2}{|\tilde{\mathbf{h}}_i^\dagger \mathbf{v}_j|^2} \right) \right] \\ &\stackrel{(b)}{\leq} 1 - E_{\mathbf{H}, \mathcal{W}} \left[\log_2 \left(|\tilde{\mathbf{h}}_i^\dagger \mathbf{v}_j|^2 \right) \right] \end{aligned} \quad (13)$$

where in (a) we consider only one of the multiuser interference terms, and (b) uses the fact that $|\tilde{\mathbf{h}}_i^\dagger \mathbf{v}_j| \leq 1$ and $|\tilde{\mathbf{h}}_i^\dagger \mathbf{v}_i| \leq 1$. By Lemma 2, $|\tilde{\mathbf{h}}_i^\dagger \mathbf{v}_j|^2$ is the product of the quantization error and a beta random variable (denoted by Y). Thus, we have

$$\begin{aligned} -E_{\mathbf{H}, \mathcal{W}} \left[\log_2 \left(|\tilde{\mathbf{h}}_i^\dagger \mathbf{v}_j|^2 \right) \right] &= -E_{\mathbf{H}, \mathcal{W}} \left[\log_2 \left(\sin^2(\angle(\tilde{\mathbf{h}}_i, \hat{\mathbf{h}}_i)) \right) \right] - E_Y [\log_2 Y] \\ &= \frac{\log_2 e}{M-1} \sum_{k=1}^{2^B} \frac{1}{k} + \log_2 e \sum_{k=1}^{M-2} \frac{1}{k} \\ &\leq \frac{B + \log_2 e}{M-1} + \log_2(M-2) + \log_2 e \end{aligned}$$

where we have used Lemma 3 as well as the easily verifiable fact that

$$E[-\log_2 Y] = (\log_2 e) \sum_{k=1}^{M-2} \frac{1}{k} \leq \log_2(M-2) + \log_2 e$$

when Y is beta $(1, M-2)$. \square

Regardless of how many feedback bits (B) are used, the system eventually becomes interference limited because interference and signal power both scale linearly with P . In Fig. 3, the performance of a five-antenna, five-user system with 10, 15, and 20 feedback bits per mobile is shown. When the SNR is small, limited feedback performs nearly as well as zero-forcing. However, as the SNR is increased, the limited feedback system becomes interference limited and the rates converge to an upper limit, as expected. Although the upper bound in Theorem 2 is quite loose in general, it does correctly predict the roughly linear dependence of the limiting throughput and B .

Notice that this interference-limited behavior can easily be avoided by serving only one user, i.e., using TDMA, but this only provides a multiplexing gain of one. However, as validated by numerical results in Section VII, TDMA is actually preferable to feedback-based zero-forcing at high SNRs if B is kept fixed.

C. Increasing Feedback Quality

In this subsection, we show that the interference-limited behavior experienced in fixed-feedback systems can be avoided by scaling the feedback rate linearly with the SNR (in decibels). In fact, if the feedback rate is scaled at the appropriate rate, the full multiplexing gain of

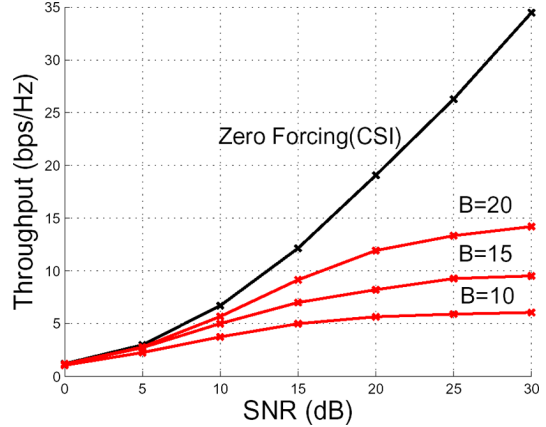


Fig. 3. 5×5 channel with fixed number of feedback bits.

M is achievable. In addition to achieving the full multiplexing gain, it is also desirable to maintain a constant rate offset $\Delta R(P)$ between the rates achievable with zero-forcing with perfect CSI and with finite-rate feedback. Note that if a bounded rate gap is maintained as SNR is taken to infinity, the full multiplexing gain is also achieved. The following theorem specifies a sufficient scaling of feedback bits to maintain a bounded rate gap.

Theorem 3: In order to maintain a rate offset no larger than $\log_2 b$ (per user) between zero-forcing with perfect CSI and with finite-rate feedback (i.e., $\Delta R(P) \leq \log_2 b \forall P$), it is sufficient to scale the number of feedback bits per mobile according to

$$B = (M-1) \log_2 P - (M-1) \log_2(b-1) \quad (14)$$

$$\approx \frac{M-1}{3} P_{\text{dB}} - (M-1) \log_2(b-1). \quad (15)$$

Proof: In order to characterize a sufficient scaling of feedback bits, we set the rate gap upper bound given in Theorem 1 equal to the maximum allowable gap of $\log_2 b$

$$\Delta R(P) < \log_2 \left(1 + P \cdot 2^{-\frac{B}{M-1}} \right) \triangleq \log_2 b.$$

By inverting this expression and solving for B as a function of b and P we get

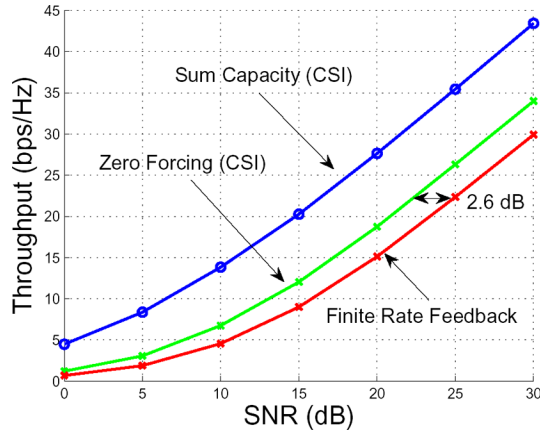
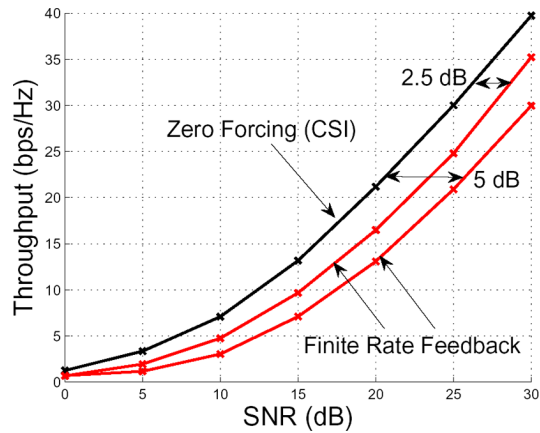
$$B = (M-1) \log_2 P - (M-1) \log_2(b-1) \quad (16)$$

$$\begin{aligned} &= \frac{(M-1) \log_2 10}{10} P_{\text{dB}} - (M-1) \log_2(b-1) \\ &\approx \frac{M-1}{3} P_{\text{dB}} - (M-1) \log_2(b-1). \end{aligned} \quad (17)$$

With this scaling of feedback bits, we clearly have $\Delta R(P) < \log_2 b$ for all P , as desired. \square

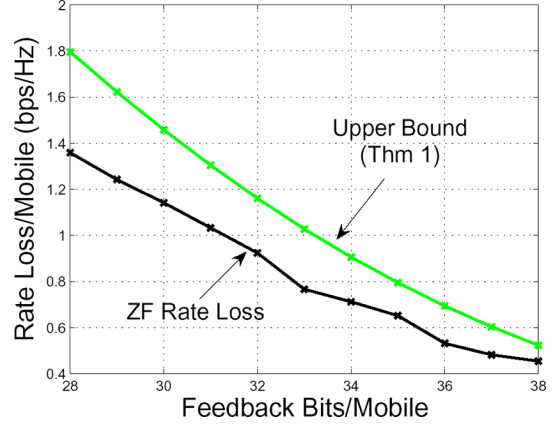
The rate offset of $\log_2 b$ (per user) can easily be translated into a power offset, which is a more useful metric from the design perspective. Since a multiplexing gain of M is achieved with zero-forcing, the zero-forcing curve has a slope of M bps/Hz/3 dB at asymptotically high SNR. Therefore, a rate offset of $\log_2 b$ bps/Hz per user, or equivalently $M \log_2 b$ bps/Hz in throughput, corresponds to a power offset of $3 \log_2 b$ decibels [33], [34]. Thus, $b = 2$ corresponds to a 1-bps/Hz rate offset per user or equivalently a 3-dB power offset. The resulting scaling of bits takes on a particularly simple form when a 3-dB offset is desired

$$B = \frac{M-1}{3} P_{\text{dB}} \text{ bits/mobile.} \quad (18)$$

Fig. 4. 5×5 channel with increasing number of feedback bits.Fig. 5. 6×6 channel with increasing number of feedback bits.

In order to achieve a smaller power offset, b needs to be made appropriately smaller. For example, a 1-dB offset corresponds to $b = 10^{1/10} = 1.259$ and thus additional $1.95(M - 1)$ feedback bits are required at all SNRs.

In Fig. 4, throughput curves are shown for a five-antenna, five-user system. The feedback load is assumed to scale according to the relationship given in (18), and limited feedback is seen to perform within 2.6 dB of perfect CSI zero-forcing. Notice that the actual power offset is smaller than 3 dB primarily due to the use of Jensen's inequality in deriving the upper bound to $\Delta R(P)$ in Theorem 1. The sum capacity, which outperforms zero-forcing by 5.55 dB in a 5×5 system [20], is also shown. In Fig. 5, throughput curves are shown for a six-antenna, six-user system. In this figure, B is scaled to guarantee a 3- and a 6-dB gaps from perfect CSIT zero-forcing (i.e., $b = 2$ and $b = 4$ in (15)). Again, the actual gaps are smaller than the bounds (2.5 and 5 dB, respectively), but are still sufficiently close to make the bounds useful. Fig. 6 plots the rate $\Delta R(P)$ in a 5×5 system at an SNR of 25 dB against the number of feedback bits, along with the upper bound from Theorem 1 that is used to derive the scaling relationship in Theorem 3. While 33.3 bits are required for the upper bound to equal 1 bps/Hz, only 31 bits are needed to have the true rate loss be equal to unity. Thus, we see that the sufficient scaling relationship given in Theorem 3 only slightly overestimates the actual required feedback rate. In addition, notice that the upper bound tracks the true rate loss quite closely, and appears to converge when B becomes large.

Fig. 6. 5×5 channel at 25 dB.

If B is scaled with SNR at a rate strictly greater than $(M - 1) \log_2 P$, i.e., $B = \alpha \log_2 P$ for any $\alpha > M - 1$, the upper bound to the rate gap (Theorem 1) is easily seen to converge to zero

$$\lim_{P \rightarrow \infty} \Delta R(P) \leq \lim_{P \rightarrow \infty} \log_2 \left(1 + P \cdot 2^{-\frac{B}{M-1}} \right) = 0$$

which implies that the actual rate gap also converges to zero. Thus, the throughput achieved with limited feedback converges (absolutely) to the perfect CSIT throughput at asymptotically high SNR under such scaling. However, scaling B at a rate slower than $(M - 1) \log_2 P$ results in a strict reduction in the multiplexing gain, as shown by the following theorem.

Theorem 4: If B is scaled as $B = \alpha \log_2 P$ for $\alpha \leq M - 1$, the throughput curve achieves a multiplexing gain of $M \left(\frac{\alpha}{M-1} \right)$.

Proof: See Appendix IV. \square

Intuitively, the signal power grows linearly with P , while the interference power scales as the product of P and the quantization error. Since the quantization error is of order $P^{-\frac{\alpha}{M-1}}$ (which is equal to $2^{-\frac{B}{M-1}}$), the interference power scales as $P^{(1-\frac{\alpha}{M-1})}$, which gives an SNR that scales as $P^{\frac{\alpha}{M-1}}$. Thus, the rate to each user is given by

$$\log \left(1 + P^{\frac{\alpha}{M-1}} \right) \approx \frac{\alpha}{M-1} \log_2 P$$

and the resulting multiplexing gain is $M \left(\frac{\alpha}{M-1} \right)$.

In Fig. 7, the throughputs achieved with feedback rates given by $B = 0.5(M - 1) \log_2 P$ and $B = 1.3(M - 1) \log_2 P$ in a 4×4 channel are shown. When $\alpha = 0.5(M - 1)$, the achieved multiplexing gain is only $0.5M = 2$, which corresponds to a slope of 2 bps/Hz per 3 dB. On the other hand, when $\alpha = 1.3(M - 1)$, the full multiplexing gain is achieved and the rate gap relative to perfect CSIT zero-forcing converges to zero at high SNR.

The required scaling of feedback with the system SNR indeed results in rather high feedback requirements in relatively high mobility environments (i.e., short coherence times). As a result, fixed-rate feedback channels may not be able to support the required loads at high SNRs. However, if the SNR on the feedback channel is the same as the downlink SNR (P), the feedback requirements may actually be feasible because the required feedback per mobile scales with $\log_2 P$, which approximates the capacity of such a reciprocal feedback channel.

D. Regularized Zero-Forcing

Although zero-forcing precoding performs very well at moderate and high SNRs, regularization can significantly increase throughput at low SNRs [27]. In fact, this is exactly analogous to the difference

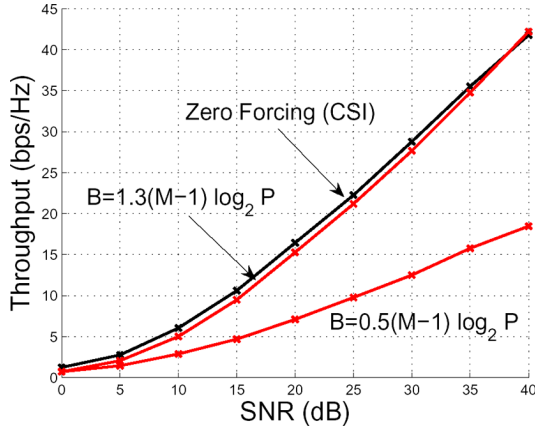


Fig. 7. Multiplexing gain as a function of feedback scaling.

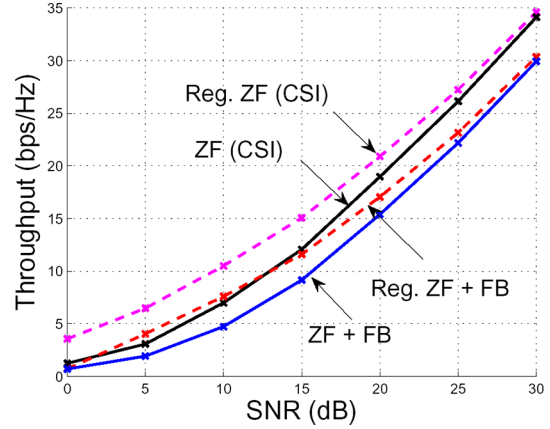
between zero-forcing equalization and minimum mean-square error (MMSE) equalization: while zero-forcing results in complete cancellation of (intersymbol) interference, an MMSE equalizer allows a measured amount of interference into the filtered output such that the output SNR is maximized. Regularized zero-forcing is also implemented through a linear precoder, but with a slightly different selection of beamforming vectors. If $\hat{\mathbf{H}}$ denotes the concatenation of quantization vectors available to the AP, the zero-forcing beamforming vectors are chosen as the normalized columns of $\hat{\mathbf{H}}^{-1}$, or equivalently of $\hat{\mathbf{H}}^\dagger (\hat{\mathbf{H}} \hat{\mathbf{H}}^\dagger)^{-1}$. With regularized zero-forcing, the beamforming vectors $\mathbf{v}_1, \dots, \mathbf{v}_K$ are chosen to be the normalized columns of the matrix

$$\hat{\mathbf{H}}^\dagger \left(\hat{\mathbf{H}} \hat{\mathbf{H}}^\dagger + \frac{M}{P} \mathbf{I} \right)^{-1}.$$

The use of the regularization constant $\frac{M}{P}$ is well motivated by results in [27] as well as the optimal MMSE filters on the dual multiple-access channel [17]. It is clear from this regularization that the regularized beamforming vectors will converge to standard zero-forcing vectors at asymptotically high SNR.

Since the rates achieved by zero-forcing and regularized zero-forcing converge at asymptotically high SNR, the feedback scaling specified in Theorem 3 gives the desired rate/power offset for regularized zero-forcing at asymptotically high SNR. Although we have not been able to extend Theorems 1 or 3 to the rate offset between regularized zero-forcing based on perfect versus feedback-based CSIT, numerical results indicate that these results actually hold at all SNRs, and not just at very high SNR values. In fact, numerical results indicate that Theorem 3 more accurately predicts the rate offset for regularized zero-forcing than for standard zero-forcing at low and moderate SNR values.

Throughput curves for zero-forcing (solid lines) and regularized zero-forcing (dotted lines) with perfect CSIT and feedback-based CSIT (with $B = \frac{M-1}{3} P_{dB}$) are shown for a 5×5 channel in Fig. 8. The throughput achieved with regularized zero-forcing with perfect CSIT is significantly larger (by approximately 4 bps/Hz) than the throughput with perfect CSIT-based zero-forcing for SNRs between 0 and 15 dB, but the two curves converge at very high SNR. The same is true for the throughput achieved with finite-rate feedback and regularized zero-forcing versus standard zero-forcing. Furthermore, while the rate offset between perfect CSIT-based zero-forcing and feedback-CSIT zero-forcing increases from nearly zero at low SNR to its limiting value at high SNR, the rate offset between the two regularized zero-forcing curves is relatively constant over the entire SNR range, as noted earlier.


 Fig. 8. 5×5 channel with regularized zero-forcing.

VI. EXTENSIONS TO GENERAL VECTOR QUANTIZATION

While the results of the previous section accurately characterize the performance of an RVQ-based zero-forcing system, it is important to determine if a system based on some optimized vector quantization codebook can significantly outperform RVQ-based systems. As the following results show, the general results from the RVQ analysis hold for any choice of quantization codebooks: fixed feedback rate systems achieve only a bounded throughput, and feedback rate must be increased proportionally to the system SNR in order to achieve the full multiplexing gain. In order to show these results, we analyze the performance of a zero-forcing/feedback-based system as described in Section IV for an arbitrary set of quantization codebooks. Thus, each mobile performs channel quantization according to some specified quantization codebook using the criterion in (2). We first establish a bound on the multiuser interference experienced as only a function of the size of each quantization codebook, and then use this bound to analyze throughput performance.

Lemma 4: Consider an arbitrary L -vector quantization codebook $\{\mathbf{w}_1, \dots, \mathbf{w}_L\}$ for mobile i , and let the random variable X_{ij} denote the interference incurred at mobile i from the beam intended for user j : $X_{ij} = |\hat{\mathbf{h}}_i^\dagger \mathbf{v}_j|^2$. For any $i \neq j$, the random variable X_{ij} stochastically dominates the random variable \tilde{X} , whose cdf is given by

$$F_{\tilde{X}}(x) = \begin{cases} L(1 - x^{M-1}), & 0 \leq x \leq 1 - \left(1 - \frac{1}{L}\right)^{\frac{1}{M-1}} \\ 1, & 1 - \left(1 - \frac{1}{L}\right)^{\frac{1}{M-1}} \leq x \leq 1 \end{cases} \quad (19)$$

or $F_{\tilde{X}}(x) \geq F_{X_{ij}}(x)$ for all $0 \leq x \leq 1$.

Proof: See Appendix V. \square

The following lemma quantifies the expectation of the logarithm of the lower bound given above, as well as its behavior if B is scaled with the SNR.

Lemma 5: The expectation of the logarithm of the random variable \tilde{X} defined in Lemma 4, i.e., $E[\log_2 \tilde{X}]$, is finite for fixed L . Furthermore, if the codebook size L is scaled with power as $B = \alpha \log_2 P$ with $L = 2^B$, the multiplexing gain of the same quantity is upper-bounded by α

$$\lim_{P \rightarrow \infty} \frac{E[-\log_2(\tilde{X})]}{\log_2 P} \leq \alpha.$$

Proof: See Appendix VI. \square

Using these lemmas, it is possible to extend the result of Theorem 2 on fixed feedback rate systems to arbitrary quantization codebooks.

Theorem 5: The throughput achieved by finite-rate feedback-based zero-forcing with arbitrary quantization codebooks of fixed size is bounded as the SNR is taken to infinity.

Proof: All steps used in the proof of Theorem 2 leading to (13) apply to arbitrary codebooks. Thus, the per user throughput for arbitrary codebooks is bounded by

$$\frac{1}{M} R_{\text{FB}}(P) \leq 1 - E_{\mathbf{H}} \left[\log_2 \left(|\hat{\mathbf{h}}_i^\dagger \mathbf{v}_j|^2 \right) \right]$$

for any $i \neq j$. Because $|\hat{\mathbf{h}}_i^\dagger \mathbf{v}_j|^2$ stochastically dominates \tilde{X} , we have

$$E \left[\log_2 \left(|\hat{\mathbf{h}}_i^\dagger \mathbf{v}_j|^2 \right) \right] \geq E[\log_2 \tilde{X}].$$

Thus, per-user throughput is bounded by $1 - E[\log_2 \tilde{X}]$, which is finite due to Lemma 5. \square

The result here is quite intuitive: because the interference power grows linearly with signal power for *any* quantization codebook, the system eventually becomes interference limited and thus has bounded throughput.

It is also possible to prove a slightly weakened version of Theorem 4 relating feedback scaling and multiplexing gain to arbitrary quantization codebooks:

Theorem 6: A finite-rate feedback-based zero-forcing system in which per-user feedback is scaled at rate $B = \alpha \log_2 P$ can achieve a multiplexing gain no larger than αM . Therefore, a necessary condition for achieving the full multiplexing gain of M is to scale feedback at least as $B = \log_2 P$.

Proof: Using steps identical to the multiplexing upper bound established in Appendix IV, the multiplexing gain m can be upper-bounded by

$$\begin{aligned} m &\leq M - \lim_{P \rightarrow \infty} \frac{ME_{\mathbf{H}, \mathbf{W}} \left[\log_2 \left(1 + \frac{P}{M} \sum_{j \neq i} |\hat{\mathbf{h}}_i^\dagger \mathbf{v}_j|^2 \right) \right]}{\log_2 P} \\ &\leq M \lim_{P \rightarrow \infty} \frac{-E[\log_2 |\hat{\mathbf{h}}_i^\dagger \mathbf{v}_j|^2]}{\log_2 P}. \end{aligned}$$

Since $E \left[\log_2 \left(|\hat{\mathbf{h}}_i^\dagger \mathbf{v}_j|^2 \right) \right] \geq E[\log_2 \tilde{X}]$ we have

$$\lim_{P \rightarrow \infty} \frac{-E[\log_2 |\hat{\mathbf{h}}_i^\dagger \mathbf{v}_j|^2]}{\log_2 P} \leq \lim_{P \rightarrow \infty} \frac{-E[\log_2 \tilde{X}]}{\log_2 P} \leq \alpha,$$

where the final inequality is due to Lemma 5. Thus, the multiplexing gain is upper-bounded by αM . \square

If RVQ is used, scaling feedback as $B = \alpha \log_2 P$ provides a multiplexing gain of $M \left(\frac{\alpha}{M-1} \right)$, and thus, $B = (M-1) \log_2 P$ is both necessary and sufficient to achieve the full multiplexing gain. If arbitrary codebooks are allowed, the preceding theorem shows that $B = \log_2 P$ is a *necessary* condition for achieving full multiplexing. Although the necessary conditions for full multiplexing do not exactly match for RVQ and arbitrary quantization codebooks (except for $M = 2$), increasing feedback linearly with $\log_2 P$, i.e., the SNR, in decibels, is required for *any* choice of quantization and thus is an inherent quality of any finite-rate feedback/zero-forcing-based system.

The gap in the pre-log term in the necessary conditions appears to be a result of the weakness of the bound on interference power given in Lemma 4 rather than due to suboptimality of RVQ. Quantization error can be shown to decrease to zero at a rate no faster than $2^{-\frac{B}{M-1}}$ (corresponding to $P^{-\frac{\alpha}{M-1}}$) by using Lemma 6, while Lemma 4 lower-bounds the rate of decrease of interference by only 2^{-B} (corresponding to $P^{-\alpha}$). We conjecture that $B = (M-1) \log_2 P$ is actually necessary

for arbitrary codebooks as well, but a more accurate bound than given in Lemma 4 is required to show this.

If each mobile uses an arbitrary quantization codebook multiplied by a random unitary matrix (i.e., performs a random and independent rotation of each of the quantization codebooks [12]), then it is not difficult to show that $B = (M-1) \log_2 P$ is indeed necessary for full multiplexing. In this scenario, the proof of Lemma 2 holds and each interference term $|\hat{\mathbf{h}}_i^\dagger \mathbf{v}_j|^2$ is equal to the product of the quantization error and a beta $(1, M-2)$ random variable. In addition, a very accurate lower bound to the quantization error of *any* vector quantization codebook has previously been established.

Lemma 6 ([35], [5]): The quantization error $\sin^2(\angle(\tilde{\mathbf{h}}_i, \hat{\mathbf{h}}_i))$ incurred by any B -bit quantization of an isotropically distributed vector stochastically dominates the random variable \tilde{Z} , whose cdf is given by

$$F_{\tilde{Z}}(z) = \begin{cases} 2^B z^{M-1}, & 0 \leq z \leq 2^{-\frac{B}{M-1}} \\ 1, & z \geq 2^{-\frac{B}{M-1}}. \end{cases} \quad (20)$$

Using these facts, we can use the framework of Theorem 3 to determine the sufficient scaling of feedback that provides a 3-dB offset from perfect CSIT for a (possibly hypothetical) system that uses *optimal* vector quantization codebooks. In order to compute this scaling, we first must compute the expectation of \tilde{Z} . A simple calculation yields

$$E[\tilde{Z}] = \int_0^1 (1 - F_{\tilde{Z}}(z)) dz = \left(\frac{M-1}{M} \right) 2^{-\frac{B}{M-1}}.$$

Notice that this differs from the upper bound to the RVQ error (Lemma 1) only in the term $\frac{M-1}{M}$, and thus, the interference power is reduced by at most a factor of $\frac{M-1}{M}$. In order to solve for the required feedback with this bound on the quantization error we set

$$\log_2 \left(1 + P \cdot \frac{M-1}{M} 2^{-\frac{B}{M-1}} \right) \triangleq \log_2 b$$

and solve for B , which gives

$$\begin{aligned} B &= (M-1) \log_2 P - (M-1) \log_2 (b-1) \\ &\quad - (M-1) \log_2 \left(\frac{M}{M-1} \right). \end{aligned} \quad (21)$$

Comparing this with the similar term for RVQ in (16), we see that the bit savings is a constant factor of $(M-1) \log_2 \left(\frac{M}{M-1} \right)$ bits at all SNRs. Furthermore, using the fact that $\log_e(1+x) \leq x$ for $x > 0$ we have

$$(M-1) \log_e \left(\frac{M}{M-1} \right) \leq 1 \text{ nat} = \log_2 e \text{ bits} \approx 1.44 \text{ bits}.$$

Thus, using RVQ leads to at most a 1.44-bit penalty relative to optimum vector quantization, which is quite small relative to the total feedback load. Of course, this is only an approximation to the suboptimality of RVQ because we have compared *sufficient* conditions on the feedback rate for RVQ-based and optimal quantization-based systems. However, numerical results indicate that the sufficient conditions provided by Theorem 3 are actually quite close to necessary conditions, and thus this comparison is in fact quite accurate.

An alternative method to measure RVQ against optimum vector quantization is to compare the performance for the same number of feedback bits, as opposed to the above analysis in which we compared the required feedback load required for identical performance. As stated earlier, the quantization error, and thus the interference, is a factor of $\frac{M-1}{M}$ smaller in the lower bound. If the feedback is scaled in order to maintain a 3-dB gap from perfect CSI zero forcing, the noise and interference term are kept bounded by two (which corresponds to 3 dB). The lower bound, on the other hand, would be $1 + \frac{M-1}{M}$ instead

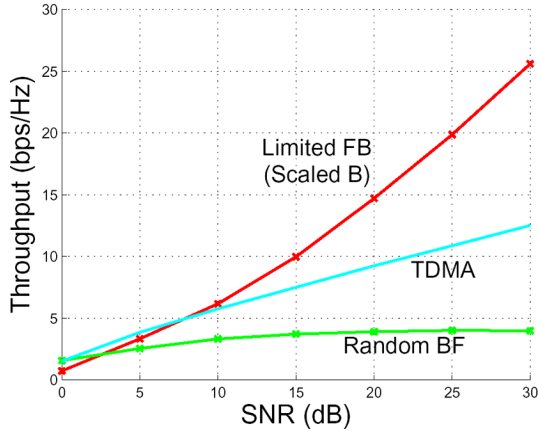


Fig. 9. 4×4 channel with scaled feedback, TDMA, and random BF.

of 2. For $M = 5$, this corresponds to 2.55 dB, or a 0.45-dB advantage relative to RVQ. As the number of transmit antennas M increases, this gap clearly goes to zero. Note that this is in accordance with results on the optimality of RVQ for large point-to-point MIMO and MISO systems [11].

VII. PERFORMANCE COMPARISON

In this section, we present numerical results comparing the throughput achieved with finite-rate feedback and two alternative transmission techniques for the MIMO downlink, random beamforming and TDMA. Because regularized zero-forcing outperforms zero-forcing at all SNRs, we only consider regularized zero-forcing systems.

Random beamforming (BF) is an extension of opportunistic beamforming [36] to the multiple-antenna downlink [7]. The transmitter randomly chooses M orthogonal beamforming vectors and transmits pilot symbols along these vectors. Each mobile measures the SINR of each beamforming vector, and feeds back the index of the vector with the highest SINR (requiring $\log_2 M$ bits), along with the corresponding SINR. The AP then transmits to the best user on each of the beamforming vectors. The required feedback per mobile is quite small ($\log_2 M$ bits plus an analog SNR value, which will presumably be sufficiently quantized), but this scheme does not perform well in systems with a moderate number of mobiles (i.e., $K \approx M$). In addition, random beamforming is interference limited at asymptotically large SNR if the number of mobiles is kept fixed.

TDMA, in which the AP serves a single user at a time, is perhaps the simplest downlink transmission scheme. We consider the TDMA throughput achievable with perfect CSIT, in which the AP transmits (using the capacity-achieving beamforming strategy) to only the user with the largest SNR. While it is possible to incorporate the effect of finite-rate feedback into a TDMA system (as described in Section III-D), the effect is relatively negligible at the feedback levels considered here and thus, for simplicity, we consider perfect CSIT. Since a TDMA system achieves a multiplexing gain of only one, we expect to see a significant throughput degradation if TDMA is used, particularly at high SNR. However, note that the difference between the sum capacity of the MIMO downlink (achieved by dirty-paper coding) and the achievable TDMA throughput is not particularly large at SNRs less than 5 or 10 dB [2].

Fig. 9 plots achievable throughput for a finite-rate feedback system with B scaled to maintain a 3-dB offset (18), TDMA, and random beamforming, in a 4×4 channel. Finite-rate feedback outperforms

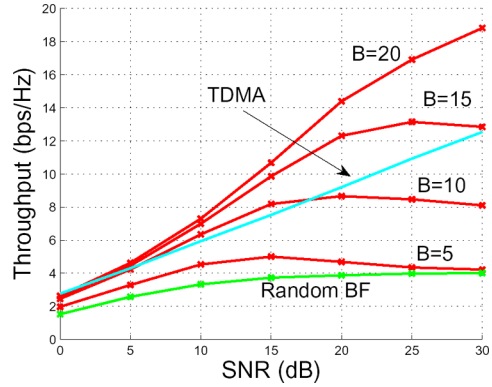


Fig. 10. 4×4 channel with fixed feedback, TDMA, and random BF.

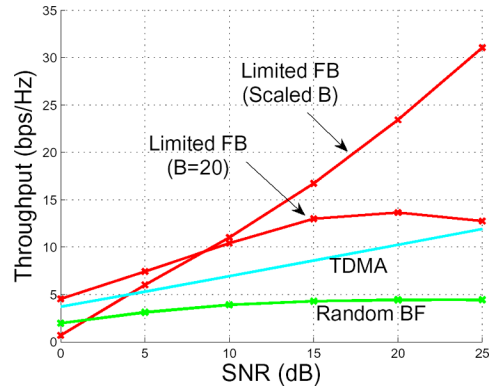


Fig. 11. 8×8 channel with feedback, TDMA, and random BF.

random BF beyond 5 dB, which is not surprising given that the feedback level per mobile (which is given by $B = P_{dB}$ for this particular channel) is significantly higher than for random BF. Finite-rate feedback and TDMA give approximately the same throughput up to 10 dB, after which the feedback system begins to significantly outperform TDMA, due to the superior multiplexing gain of the zero-forcing system. The same channel is considered in Fig. 10, but with fixed feedback levels ($B = 5, 10, 15, 20$) in the finite-rate feedback system.⁵ Here we see that TDMA is a better choice than finite-rate feedback with either 5 or 10 bits of feedback per mobile. If 15 or 20 feedback bits are permitted, however, finite-rate feedback can provide a significant advantage over TDMA, particularly above 10 dB.

Fig. 11 displays achievable throughput in an 8×8 channel for finite-rate feedback systems with B scaled according to (18) and with $B = 20$, along with TDMA and random BF throughputs. The throughput achieved with scaled feedback is considerably larger than the TDMA throughput, due to the large number of spatial degrees of freedom used by the zero-forcing system. The 20 feedback bit system outperforms TDMA at moderate SNRs, but hits the interference limited regime around 15 or 20 dB.

In general, finite-rate feedback-based zero-forcing outperforms TDMA at SNRs above 5 or 10 dB if the feedback per mobile is sufficiently large, but does not provide a significant advantage at low SNRs. Furthermore, random beamforming is outperformed by both TDMA and finite-rate feedback at essentially all SNR levels. However, this is largely due to the limited number of mobiles, as

⁵Note that the finite-rate feedback throughput decreases with SNR in some cases due to the decreasing regularization factor as a function of the SNR. A more careful tuning of this parameter can prevent this behavior, but does not significantly increase throughput.

random beamforming does provide excellent performance in systems with many more mobiles than AP antennas.

VIII. CONCLUSION

The use of multiuser MIMO techniques can significantly increase downlink throughput without requiring large numbers of antennas at each mobile device. However, it is crucial that the transmitter have accurate CSI in order to realize these gains. In fact, the availability of CSI appears to be the critical issue that will determine the feasibility of multiuser MIMO techniques in future wireless communication systems.

We investigated the finite-rate feedback model, in which each mobile quantizes its channel realization to a finite number of bits that are fed back to the transmitter. Although this model has been extensively studied for point-to-point MIMO channels, conclusions are quite different in the multiuser setting. Our primary result showed that the number of feedback bits per mobile must be increased linearly with the SNR (in decibels) in order to achieve the full multiplexing gain of the channel if zero-forcing precoding is performed on the basis of the channel feedback. As a result of this, feedback levels are quite high in MIMO downlink channels: in a four-antenna system, for example, each mobile must feed back 10 bits at an overall system SNR of 10 dB. In contrast, feedback does not need to scale with SNR in point-to-point MIMO systems, and even a relatively small number of bits (e.g., 4 or 5) can be very beneficial at all SNR levels.

The intuition for the extreme sensitivity of the MIMO downlink channel to imperfection in CSIT, as compared to point-to-point MIMO channels, is relatively straightforward. In point-to-point MIMO channels, imperfect CSIT leads to mismatch between the input and the transmission modes of the channel and thus some “wasted” transmission power (i.e., power that is transmitted into the nullspace of the channel), which reduces the received SNR but has no other deleterious effect. In a MIMO downlink channel, imperfect CSIT also leads to mismatch between the input and the channel, but the effect is considerably stronger because all misdirected transmission leads to increased multiuser interference, which is significantly more harmful than a reduction in desired signal power.

Although feedback requirements are quite stringent, there are a number of reasons to be optimistic regarding CSI feedback in downlink channels. First, note that we have considered only the most basic i.i.d. Rayleigh block-fading model, and feedback rates can surely be decreased by exploiting spatial and temporal correlation inherent in any physical fading process, as has already been extensively studied for point-to-point MIMO channels [37]–[40]. Furthermore, recent work has shown that a small number of mobile antennas can be used to significantly improve quantization quality and thereby decrease the required feedback rates [41]. In addition, it may also be possible to exploit multiuser diversity effects and thereby reduce feedback rates in systems with a large number of mobiles [7], [14], [9]. Within this body of work, one interesting idea is to have only a subset of mobiles (e.g., mobiles meeting some SNR threshold) feed back their channel information [42], [43], [9]. While this technique can significantly reduce the total number of feedback bits to be transmitted, it also requires contention-based feedback (i.e., random access), which can lead to throughput reduction as well as additional latency on the feedback channels. Although we have considered only digital feedback methods, analog feedback appears to have a number of attractive properties for the downlink channel [13], [44]–[46]. Finally, if the feedback channel from each of the mobiles has the same SNR as the downlink channel, which may be reasonable in certain scenarios, then the required feedback levels may be supportable if near-capacity signaling is used over the feedback channel.

We close by mentioning a few important issues not considered in this work. One key assumption made in this work is that the channel

feedback is *instantaneous*. Of course, there will be some nonzero delay associated with transmitting feedback bits from the mobiles to the AP, and this delay can be quite significant in fast fading (large Doppler spread) channels. In fact, results in [46] indicate that feedback delay can severely limit the performance of certain downlink transmission schemes at even moderate levels of Doppler. In addition, each mobile is assumed to have perfect CSI, while there will be nonzero receiver estimation error in any practical system. This will clearly lead to additional imperfection in the CSI provided to the AP, and could have significant effects. Frequency-selective channels also require attention; consider related work on frequency-selective point-to-point MIMO channels [47], [48]. Furthermore, note that we have only considered FDD systems. Channel reciprocity can be exploited to acquire downlink channel state information from the uplink in time-division duplexed (TDD) channels, although recent results indicate that, somewhat counter-intuitively, TDD may in fact be less attractive than FDD from a channel state information perspective [44]. Many of the tools used here appear to be well suited to analyze the effect of imperfect CSIT in TDD systems as well. Finally, we note that the analysis performed here applies only to linear precoding strategies. Determining how far the proposed achievability scheme is from the true capacity of the MIMO downlink channel with imperfect CSIT is a challenging unsolved information-theoretic problem.

APPENDIX I EXPECTED QUANTIZATION ERROR

In this appendix, we provide an alternative proof for the closed-form representation of the expected quantization error. The following integral representation for the beta function is given in [49, p. 5]:

$$\beta\left(c, \frac{a}{b}\right) = b \int_0^1 z^{a-1} (1-z)^{c-1} dz, \quad a > 0, b > 0, c > 0.$$

With $a = 1$, $b = M - 1$, and $c = 2^B + 1$ this yields

$$\beta\left(2^B + 1, \frac{1}{M-1}\right) = (M-1) \int_0^1 (1-z)^{2^B} dz.$$

Using the fact that $\Pr\left(\sin^2\left(\angle(\tilde{\mathbf{h}}_i, \hat{\mathbf{h}}_i)\right) \geq z\right) = (1-z)^{M-1} 2^{2^B}$, we have

$$\begin{aligned} E_{\mathbf{H}, \mathcal{W}} \left[\sin^2 \left(\angle(\tilde{\mathbf{h}}_i, \hat{\mathbf{h}}_i) \right) \right] &= \int_0^1 (1-z)^{M-1} 2^{2^B} dz \\ &= \frac{1}{M-1} \beta\left(2^B + 1, \frac{1}{M-1}\right) \\ &= \frac{\frac{1}{M-1} \Gamma(2^B + 1) \Gamma\left(\frac{1}{M-1}\right)}{\Gamma\left(2^B + 1 + \frac{1}{M-1}\right)} \\ &= \frac{2^{2^B} \Gamma(2^B) \Gamma\left(1 + \frac{1}{M-1}\right)}{\Gamma\left(2^B + 1 + \frac{1}{M-1}\right)} \\ &= 2^{2^B} \cdot \beta\left(2^B, \frac{M}{M-1}\right) \end{aligned}$$

where we have used the fundamental equality $\Gamma(z+1) = z\Gamma(z)$.

APPENDIX II PROOF OF LEMMA 1

The expected quantization error is given by [29]

$$E_{\mathbf{H}, \mathcal{W}} \left[\sin^2 \left(\angle(\tilde{\mathbf{h}}_i, \hat{\mathbf{h}}_i) \right) \right] = 2^{2^B} \cdot \beta\left(2^B, \frac{M}{M-1}\right). \quad (22)$$

For $M = 2$, we have

$$\begin{aligned} 2^B \cdot \beta\left(2^B, 2\right) &= \frac{2^B \Gamma(2^B) \Gamma(2)}{\Gamma(2^B + 2)} \\ &= \frac{(2^B)!}{(2^B + 1)!} \\ &= (2^B + 1)^{-1} \\ &< 2^{-B}. \end{aligned}$$

For $M > 2$

$$\begin{aligned} 2^B \cdot \beta\left(2^B, \frac{M}{M-1}\right) &= 2^B \frac{\Gamma(2^B) \Gamma\left(1 + \frac{1}{M-1}\right)}{\Gamma\left(2^B + 1 + \frac{1}{M-1}\right)} \\ &\leq \frac{2^B \Gamma(2^B)}{\Gamma\left(2^B + 1 + \frac{1}{M-1}\right)} \\ &= \frac{\Gamma(2^B + 1)}{\Gamma\left(2^B + 1 + \frac{1}{M-1}\right)}. \end{aligned}$$

The preceding inequality is reached because $\Gamma(x) \leq 1$ for $1 \leq x \leq 2$, due to the convexity of the gamma function [30] and the fact that $\Gamma(1) = \Gamma(2) = 1$. By applying Kershaw's inequality for the gamma function [50]

$$\frac{\Gamma(x+s)}{\Gamma(x+1)} < \left(x + \frac{s}{2}\right)^{s-1}, \quad \forall x > 0, 0 < s < 1$$

with $x = 2^B + \frac{1}{M-1}$ and $s = 1 - \frac{1}{M-1}$ we get

$$\frac{\Gamma(2^B + 1)}{\Gamma\left(2^B + 1 + \frac{1}{M-1}\right)} < \left(2^B + \frac{M}{2(M-1)}\right)^{-\frac{1}{M-1}}.$$

Furthermore, the decreasing nature of the function $(\cdot)^{-\frac{1}{M-1}}$ gives a further upper bound of $2^{-\frac{B}{M-1}}$.

APPENDIX III PROOF OF LEMMA 3

Let $Z = \sin^2(\angle(\tilde{\mathbf{h}}_i, \hat{\mathbf{h}}_i))$ represent the quantization error. As stated in Section III-C, Z is the minimum of 2^B beta $(M-1, 1)$ random variables with cdf given by $\Pr(Z \geq z) = (1 - z^{M-1})^L$, where $L = 2^B$. We wish to compute $E[\log_e Z]$, or equivalently $E[-\log_e Z]$. Since $0 \leq Z \leq 1$, the random variable $-\log_e Z$ is nonnegative with support $[0, \infty)$. Using the fact that $E[X] = \int_0^\infty \Pr(X \geq x) dx$ for nonnegative random variables and the binomial expansion, we have

$$\begin{aligned} E[-\log_e Z] &= \int_0^\infty \Pr(Z \leq e^{-z}) dz \\ &= \int_0^\infty 1 - (1 - e^{-z(M-1)})^L dz \\ &= \int_0^\infty 1 - \sum_{k=0}^L \binom{L}{k} (-1)^k e^{-z(M-1)k} dz \\ &= \int_0^\infty \sum_{k=1}^L \binom{L}{k} (-1)^{k+1} e^{-z(M-1)k} dz \\ &= \frac{1}{M-1} \sum_{k=1}^L \binom{L}{k} \frac{(-1)^{k+1}}{k} \\ &= \frac{1}{M-1} \sum_{k=1}^L \frac{1}{k} \end{aligned}$$

where the final line follows from [51, Sec. 0.155].

Furthermore, since $\log_e a = \int_1^a \frac{1}{x} dx$, we have

$$\log_e L \leq \sum_{k=1}^L \frac{1}{k} \leq \log_e L + 1.$$

We multiply by $\log_2 e$ to translate to base 2, and thus get

$$E[-\log_2 Z] = \frac{\log_2 e}{M-1} \sum_{k=1}^L \frac{1}{k}.$$

Using $L = 2^B$ we get the subsequent bounds.

APPENDIX IV PROOF OF THEOREM 4

The multiplexing gain can be expanded as

$$\begin{aligned} m &\triangleq \lim_{P \rightarrow \infty} \frac{ME_{\mathbf{H},W}[R_{\text{FB}}(P)]}{\log_2 P} \\ &= \lim_{P \rightarrow \infty} \frac{ME_{\mathbf{H},W}\left[\log_2\left(1 + \frac{P}{M} |\mathbf{h}_i^\dagger \mathbf{v}_i|^2 + \frac{P}{M} \sum_{j \neq i} |\mathbf{h}_i^\dagger \mathbf{v}_j|^2\right)\right]}{\log_2 P} \\ &\quad - \lim_{P \rightarrow \infty} \frac{ME_{\mathbf{H},W}\left[\log_2\left(1 + \frac{P}{M} \sum_{j \neq i} |\mathbf{h}_i^\dagger \mathbf{v}_j|^2\right)\right]}{\log_2 P} \\ &= M - \lim_{P \rightarrow \infty} \frac{ME_{\mathbf{H},W}\left[\log_2\left(1 + \frac{P}{M} \sum_{j \neq i} |\mathbf{h}_i^\dagger \mathbf{v}_j|^2\right)\right]}{\log_2 P}. \end{aligned} \quad (23)$$

The final step follows because the quantity

$$\log_2\left(1 + \frac{P}{M} |\mathbf{h}_i^\dagger \mathbf{v}_i|^2 + \frac{P}{M} \sum_{j \neq i} |\mathbf{h}_i^\dagger \mathbf{v}_j|^2\right)$$

is lower-bounded by $\log_2\left(1 + \frac{P}{M} |\mathbf{h}_i^\dagger \mathbf{v}_i|^2\right)$ and is upper-bounded by $\log_2(1 + P \|\mathbf{h}_i\|^2)$, and the multiplexing gain of the upper and lower bounds are easily shown to be one.

We first show that $m \leq \frac{\alpha}{M-1}$ (using $L = 2^B = P^\alpha$)

$$\begin{aligned} E_{\mathbf{H},W}\left[\log_2\left(1 + \frac{P}{M} \sum_{j \neq i} |\mathbf{h}_i^\dagger \mathbf{v}_j|^2\right)\right] &\geq E_{\mathbf{H},W}\left[\log_2\left(\frac{P}{M} |\mathbf{h}_i^\dagger \mathbf{v}_j|^2\right)\right] \\ &= \log_2\left(\frac{P}{M}\right) + E_{\mathbf{H}}[\log_2 \|\mathbf{h}_i\|^2] + E_{\mathbf{H},W}\left[\log_2 |\hat{\mathbf{h}}_i^\dagger \mathbf{v}_j|^2\right] \\ &= \log_2 P + E_{\mathbf{H},W}\left[\log_2\left(\sin^2(\angle(\tilde{\mathbf{h}}_i, \hat{\mathbf{h}}_i))\right)\right] + O(1) \\ &= -\log_2 P - \frac{\log_2 e}{M-1} \sum_{k=1}^L \frac{1}{k} + O(1) \\ &\geq \log_2 P - \frac{1}{M-1} \log_2 L + O(1) \\ &= \left(1 - \frac{\alpha}{M-1}\right) \log_2 P + O(1) \end{aligned}$$

where we have used Lemma 3 to evaluate the expectation of the logarithm of the interference term. Plugging this bound in to (23) gives $m \leq M \left(\frac{\alpha}{M-1}\right)$.

To show $m \geq M \left(\frac{\alpha}{M-1} \right)$, we upper-bound the limit in (23) using the fact that $|\tilde{\mathbf{h}}_i^\dagger \mathbf{v}_j|^2 \leq \sin^2(\tilde{\mathbf{h}}_i, \hat{\mathbf{h}}_i)$ for any $i \neq j$ (from (12)) and Jensen's inequality

$$\begin{aligned} & E_{\mathbf{H}, \mathbf{W}} \left[\log_2 \left(1 + \frac{P}{M} \sum_{j \neq i} \|\mathbf{h}_i\|^2 |\tilde{\mathbf{h}}_i^\dagger \mathbf{v}_j|^2 \right) \right] \\ & \leq E_{\mathbf{H}, \mathbf{W}} \left[\log_2 \left(1 + \frac{P}{M} (M-1) \|\mathbf{h}_i\|^2 \sin^2(\tilde{\mathbf{h}}_i, \hat{\mathbf{h}}_i) \right) \right] \\ & \leq \log_2 \left(1 + P(M-1) E \left[\sin^2(\tilde{\mathbf{h}}_i, \hat{\mathbf{h}}_i) \right] \right) \\ & \leq \log_2 \left(1 + P(M-1) 2^{-\frac{B}{M-1}} \right) \\ & = \log_2 \left(1 + (M-1) P^{(1-\frac{\alpha}{M-1})} \right). \end{aligned}$$

Thus, we have

$$\lim_{P \rightarrow \infty} \frac{ME_{\mathbf{H}, \mathbf{W}} \left[\log_2 \left(1 + \frac{P}{M} \sum_{j \neq i} |\mathbf{h}_i^\dagger \mathbf{v}_j|^2 \right) \right]}{\log_2 P} \leq M \left(1 - \frac{\alpha}{M-1} \right)$$

which gives $m \geq M \left(\frac{\alpha}{M-1} \right)$.

APPENDIX V PROOF OF LEMMA 4

Without loss of generality, consider $i = 1$ and $j = 2$, i.e., $X_{12} = |\tilde{\mathbf{h}}_1^\dagger \mathbf{v}_2|^2$. To prove the bound, we first condition on the quantizations of users 3 through M , i.e., $\tilde{\mathbf{h}}_3, \dots, \tilde{\mathbf{h}}_M$, or equivalently, we condition on their channel realizations. Since the beamforming vector \mathbf{v}_2 is a function of the quantizations of user 1 and users 3, \dots, M , \mathbf{v}_2 is a deterministic function of $\hat{\mathbf{h}}_1$ due to the conditioning. Let $\mathcal{V}(\mathbf{w}_i)$ correspond to the Voronoi region of quantization vector \mathbf{w}_i , i.e., the set of channel directions $\hat{\mathbf{h}}_1$ quantized to \mathbf{w}_i . Furthermore, let $\mathbf{v}(\mathbf{w}_i)$ be the beamforming vector for user 2 when $\hat{\mathbf{h}}_1 \in \mathcal{V}(\mathbf{w}_i)$. The beamforming vector is chosen exactly orthogonal to the quantization \mathbf{w}_i , but the interference term $X_{12} = |\tilde{\mathbf{h}}_1^\dagger \mathbf{v}_2|^2$ is small only if the actual channel direction $\hat{\mathbf{h}}_1$, which is presumably close to the quantization vector \mathbf{w}_i , is also nearly orthogonal to \mathbf{v}_2 . To be more precise, the set of realizations in $\mathcal{V}(\mathbf{w}_i)$ that correspond to $X_{12} \leq x$ are the directions $\tilde{\mathbf{h}}_1$ in the set

$$\mathcal{V}(\mathbf{w}_i) \cap \{\mathbf{s} : |\mathbf{v}(\mathbf{w}_i)^\dagger \mathbf{s}|^2 \leq x\}.$$

The probability that $X_{12} \leq x$ is therefore given by the area of the union of all such regions, where the union is taken across the L Voronoi regions

$$\begin{aligned} & \Pr(X_{12} \leq x | \tilde{\mathbf{h}}_3, \dots, \tilde{\mathbf{h}}_M) \\ & = A \left(\bigcup_{i=1}^L \left(\mathcal{V}(\mathbf{w}_i) \cap \{\mathbf{s} : \|\mathbf{s}\| = 1, |\mathbf{v}(\mathbf{w}_i)^\dagger \mathbf{s}|^2 \leq x\} \right) \right) \\ & \leq A \left(\bigcup_{i=1}^L \{\mathbf{s} : \|\mathbf{s}\| = 1, |\mathbf{v}(\mathbf{w}_i)^\dagger \mathbf{s}|^2 \leq x\} \right) \\ & \leq \sum_{i=1}^L A \left(\{\mathbf{s} : \|\mathbf{s}\| = 1, |\mathbf{v}(\mathbf{w}_i)^\dagger \mathbf{s}|^2 \leq x\} \right) \end{aligned}$$

where $A(\cdot)$ refers to the fraction of the area of the surface of the unit sphere. Using the $\beta(1, M-1)$ distribution it is straightforward to compute

$$A \left(\{\mathbf{s} : \|\mathbf{s}\| = 1, |\mathbf{v}(\mathbf{w}_i)^\dagger \mathbf{s}|^2 \leq x\} \right) = 1 - (1-x)^{M-1}.$$

Therefore, we have $\Pr(X_{12} \leq x | \tilde{\mathbf{h}}_3, \dots, \tilde{\mathbf{h}}_M) \leq L(1 - (1-x)^{M-1})$ for all $0 \leq x \leq 1$. Since this bound does not depend on the conditioning, it holds unconditionally as well: $\Pr(X_{12} \leq x) \leq L(1 - (1-x)^{M-1})$. Combining this with $\Pr(X_{12} \leq x) \leq 1$, we get the result.

APPENDIX VI PROOF OF LEMMA 5

Since $0 \leq \tilde{X} \leq 1$, $\log_e \tilde{X} \leq 0$, and thus

$$E[-\log_e \tilde{X}] = \int_0^\infty \Pr(-\log_e \tilde{X} \geq x) dx.$$

Denoting $c = -\log_e \left(1 - \left(1 - \frac{1}{L} \right)^{\frac{1}{M-1}} \right)$, we have

$$\begin{aligned} E[-\log_e \tilde{X}] & = \int_0^\infty \Pr(\tilde{X} \leq e^{-x}) dx \\ & = c + \int_c^\infty L(1 - (1 - e^{-x})^{M-1}) dx. \end{aligned} \quad (24)$$

Evaluating the integral expression, we get

$$\begin{aligned} & \int_c^\infty L(1 - (1 - e^{-x})^{M-1}) dx \\ & \stackrel{(a)}{=} L \int_c^\infty 1 - \sum_{k=0}^{M-1} \binom{M-1}{k} (-1)^{k+1} e^{-xk} dx \\ & = L \sum_{k=1}^{M-1} \binom{M-1}{k} (-1)^k \int_c^\infty e^{-xk} dx \\ & \stackrel{(b)}{\leq} L \sum_{k=1}^{M-1} \binom{M-1}{k} \int_c^\infty e^{-x} dx \\ & = L \sum_{k=1}^{M-1} \binom{M-1}{k} e^{-c} \end{aligned} \quad (25)$$

where (a) follows from the binomial expansion and (b) holds because $e^{-x} \geq e^{-kx}$ for all $k \geq 1, x \geq 0$, and each of the terms in the new sum is nonnegative. Plugging this expression into (24) and using the finiteness of c , we clearly see that the expectation is finite.

To bound the multiplexing gain, first consider the constant c . Using the basic property $x \geq x^p$ for all $x \geq 0, p \leq 1$ we have

$$\left(1 - \frac{1}{L} \right)^{\frac{1}{M-1}} \leq 1 - \frac{1}{L}.$$

With some simple arithmetic, this yields

$$c \leq \log_e L.$$

Next, let us upper-bound the second term in (24). Starting with the upper bound given in (25) we have

$$\begin{aligned} & \int_c^\infty L(1 - (1 - e^{-x})^{M-1}) dx \\ & \leq L \sum_{k=1}^{M-1} \binom{M-1}{k} e^{-c} \\ & = \sum_{k=1}^{M-1} \binom{M-1}{k} L \left(1 - \left(1 - \frac{1}{L} \right)^{\frac{1}{M-1}} \right). \end{aligned}$$

Applying the convergent power series

$$(1+x)^q = 1 + qx + \frac{q(q-1)}{2!}x^2 + \dots + \frac{q(q-1)\dots(q-k+1)}{k!}x^k + \dots$$

[51] to $(1 - 1/L)^{M-1}$ we have

$$\begin{aligned} & 1 - \left(1 - \frac{1}{L}\right)^{\frac{1}{M-1}} \\ &= 1 - \left(1 - \frac{1}{M-1} \frac{1}{L} + \frac{1}{2!} \frac{1}{M-1} \frac{2-M}{M-1} \left(\frac{1}{L}\right)^2 + \dots\right) \\ &= \frac{1}{M-1} \frac{1}{L} + a_2 \left(\frac{1}{L}\right)^2 + a_3 \left(\frac{1}{L}\right)^3 + \dots, \end{aligned}$$

where each of the constants a_2, a_3, \dots are nonnegative and easily verified to be less than unity. Thus, we have

$$\begin{aligned} L \left(1 - \left(1 - \frac{1}{L}\right)^{\frac{1}{M-1}}\right) &= \frac{1}{M-1} + a_2 \left(\frac{1}{L}\right) + a_3 \left(\frac{1}{L}\right)^2 + \dots \\ &\leq \frac{1}{M-1} + \sum_{k=1}^{\infty} L^{-k} \\ &= \frac{1}{M-1} + \frac{1}{L-1}. \end{aligned}$$

Plugging these upper bounds into (24) then gives

$$E[-\log_e \tilde{X}] \leq \log_e L + \left(\frac{1}{M-1} + \frac{1}{L-1}\right) \sum_{k=1}^{M-1} \binom{M-1}{k}.$$

Since $L = 2^B = P^\alpha$, the second term converges to a constant as P and L go to infinity, and therefore,

$$\lim_{P \rightarrow \infty} \frac{E[-\log_e \tilde{X}]}{\log_e P} \leq \alpha.$$

ACKNOWLEDGMENT

The author would like to thank David Love for discussions and for providing a preprint of [29]. In addition, the author acknowledges useful discussions with Georgios Giannakis, Syed Ali Jafar, Taesang Yoo, Giuseppe Caire, and Mari Kobayashi on limited feedback systems.

REFERENCES

[1] G. Caire and S. Shamai (Shitz), "On the achievable throughput of a multiantenna Gaussian broadcast channel," *IEEE Trans. Inf. Theory*, vol. 49, no. 7, pp. 1691–1706, Jul. 2003.
 [2] N. Jindal and A. Goldsmith, "Dirty paper coding versus TDMA for MIMO broadcast channels," *IEEE Trans. Inf. Theory*, vol. 51, no. 5, pp. 1783–1794, May 2005.
 [3] A. Narula, M. J. Lopez, M. D. Trott, and G. W. Wornell, "Efficient use of side information in multiple antenna data transmission over fading channels," *IEEE J. Select. Areas Commun.*, vol. 16, no. 8, pp. 1423–1436, Oct. 1998.
 [4] D. Love, R. Heath, and T. Strohmer, "Grassmannian beamforming for multiple-input multiple-output wireless systems," *IEEE Trans. Inf. Theory*, vol. 49, no. 10, pp. 2735–2747, Oct. 2003.
 [5] K. Mukkavilli, A. Sabharwal, E. Erkip, and B. Aazhang, "On beamforming with finite rate feedback in multiple-antenna systems," *IEEE Trans. Inf. Theory*, vol. 49, no. 10, pp. 2562–2579, Oct. 2003.
 [6] D. Love, R. Heath, W. Santipach, and M. Honig, "What is the value of limited feedback for MIMO channels?," *IEEE Commun. Mag.*, vol. 42, no. 10, pp. 54–59, Oct. 2004.

[7] M. Sharif and B. Hassibi, "On the capacity of MIMO broadcast channels with partial side information," *IEEE Trans. Inf. Theory*, vol. 51, no. 2, pp. 506–522, Feb. 2005.
 [8] T. Yoo and A. Goldsmith, "On the optimality of multiantenna broadcast scheduling using zero-forcing beamforming," *IEEE J. Select. Areas Commun.*, vol. 24, no. 3, pp. 528–541, Mar. 2006.
 [9] C. Swannack, E. Uysal-Biyikoglu, and G. Wornell, "MIMO broadcast scheduling with limited channel state information," in *Proc. 43rd Allerton Conf. Communications, Control, and Computing*, Monticello, IL, Oct. 2005.
 [10] W. Santipach and M. Honig, "Signature optimization for CDMA with limited feedback," *IEEE Trans. Inf. Theory*, vol. 51, no. 10, pp. 3475–3492, Oct. 2005.
 [11] —, "Asymptotic capacity of beamforming with limited feedback," in *Proc. IEEE Int. Symp. Information Theory*, Chicago, IL, Jun./Jul. 2004, p. 290.
 [12] P. Ding, D. Love, and M. Zoltowski, "Multiple antenna broadcast channels with shape feedback and limited feedback," *IEEE Trans. Signal Process.*, accepted for publication.
 [13] D. Samardzija and N. B. Mandayam, "Unquantized and uncoded channel state information feedback in multiple antenna multiuser systems," *IEEE Trans. Commun.*, vol. 54, no. 7, pp. 1335–1345, Jul. 2006.
 [14] T. Yoo, N. Jindal, and A. Goldsmith, "Finite rate feedback MIMO broadcast channels with a large number of users," in *Proceedings IEEE Int. Symp. Information Theory*, Seattle, WA, Jul. 2006, pp. 1214–1218.
 [15] H. Weingarten, Y. Steinberg, and S. Shamai (Shitz), "The capacity region of the Gaussian multiple-input multiple-output broadcast channel," *IEEE Trans. Inf. Theory*, vol. 52, no. 9, pp. 3936–3964, Sep. 2006.
 [16] S. Vishwanath, N. Jindal, and A. Goldsmith, "Duality, achievable rates, and sum-rate capacity of MIMO broadcast channels," *IEEE Trans. Inf. Theory*, vol. 49, no. 10, pp. 2658–2668, Oct. 2003.
 [17] P. Viswanath and D. N. C. Tse, "Sum capacity of the vector Gaussian broadcast channel and uplink-downlink duality," *IEEE Trans. Inf. Theory*, vol. 49, no. 8, pp. 1912–1921, Aug. 2003.
 [18] W. Yu and J. M. Cioffi, "Sum capacity of Gaussian vector broadcast channels," *IEEE Trans. Inf. Theory*, vol. 50, no. 9, pp. 1875–1892, Sep. 2004.
 [19] M. Costa, "Writing on dirty paper," *IEEE Trans. Inf. Theory*, vol. IT-29, no. 3, pp. 439–441, May 1983.
 [20] N. Jindal, "A high SNR analysis of MIMO broadcast channels," in *Proc. IEEE Int. Symp. Information Theory*, Adelaide, Australia, Sep. 2005, pp. 2310–2314.
 [21] T. Cover, "Broadcast channels," *IEEE Trans. Inf. Theory*, vol. IT-18, no. 1, pp. 2–14, Jan. 1972.
 [22] S. Jafar and A. Goldsmith, "Isotropic fading vector broadcast channels: The scalar upperbound and loss in degrees of freedom," *IEEE Trans. Inf. Theory*, vol. 51, no. 3, pp. 848–857, Mar. 2005.
 [23] A. Lapidoth, S. Shamai (Shitz), and M. Wigger, "On the capacity of a MIMO fading broadcast channel with imperfect transmitter side-information," in *Proc. 43rd Allerton Conf. Communications, Control, and Computing*, Monticello, IL, Sep. 2005.
 [24] R. Zamir, S. Shamai (Shitz), and U. Erez, "Nested linear/lattice codes for structured multiterminal binning," *IEEE Trans. Inf. Theory*, vol. 48, no. 6, pp. 1250–1276, Jun. 2002.
 [25] S. ten Brink and U. Erez, "A close-to-capacity dirty paper coding scheme," in *Proc. IEEE Int. Symp. Information Theory*, Chicago, IL, Jun./Jul. 2004, p. 533.
 [26] T. Philosof, U. Erez, and R. Zamir, "Combined shaping and precoding for interference cancellation at low SNR," in *Proc. IEEE Int. Symp. Inform. Theory*, Yokohama, Japan, Jun./Jul. 2003, p. 68.
 [27] C. Peel, B. Hochwald, and A. Swindlehurst, "Vector-perturbation technique for near-capacity multiantenna multiuser communication-Part I: Channel inversion and regularization," *IEEE Trans. Commun.*, vol. 53, no. 1, pp. 195–202, Jan. 2005.
 [28] F. Boccardi, F. Tosato, and G. Caire, "Precoding schemes for the MIMO-GBC," in *Proc. f Int. Zurich Seminar on Communications*, Zurich, Switzerland, Feb. 2006, pp. 10–13.
 [29] C. Au-Yeung and D. J. Love, "On the performance of random vector quantization limited feedback beamforming in a MISO system," *IEEE Trans. Wireless Commun.*, to be published.
 [30] J. P. Davis, "Leonhard Euler's integral: A historical profile of the gamma function," *Amer. Math. Monthly*, vol. 66, no. 10, pp. 849–869, Dec. 1959.
 [31] I. E. Telatar, "Capacity of multi-antenna Gaussian channels," *Europ. Trans. Telecomm.*, vol. 10, no. 6, pp. 585–596, Nov. 1999.
 [32] S. A. Jafar and S. Srinivasa, "On the optimality of beamforming with quantized feedback," *IEEE Trans. Inf. Theory*, submitted for publication.

- [33] S. Shamai (Shitz) and S. Verdú, "The impact of frequency-flat fading on the spectral efficiency of CDMA," *IEEE Trans. Inf. Theory*, vol. 47, no. 4, pp. 1302–1327, May 2001.
- [34] A. Lozano, A. Tulino, and S. Verdú, "High-SNR power offset in multi-antenna communication," *IEEE Trans. Inf. Theory*, vol. 51, no. 12, pp. 4134–4151, Dec. 2005.
- [35] S. Zhou, Z. Wang, and G. Giannakis, "Quantifying the power loss when transmit beamforming relies on finite rate feedback," *IEEE Trans. Wireless Commun.*, vol. 4, no. 4, pp. 1948–1957, Apr. 2005.
- [36] P. Viswanath, D. N. C. Tse, and R. Laroia, "Opportunistic beamforming using dumb antennas," *IEEE Trans. Inf. Theory*, vol. 48, no. 6, pp. 1277–1294, Jun. 2002.
- [37] D. Love and R. Heath, "Grassmannian beamforming on correlated MIMO channels," in *Proc. IEEE Globecom*, Dallas, TX, Nov. 2004, vol. 1, pp. 106–110.
- [38] P. Xia and G. B. Giannakis, "Design and analysis of transmit-beamforming based on limited-rate feedback," in *Proc. IEEE Vehicular Technology Conf.*, Los Angeles, CA, Sep. 2004, vol. 3, pp. 1653–1657.
- [39] V. Raghavan, A. Sayeed, and N. Boston, "Near-optimal codebook constructions for limited-feedback beamforming in correlated MIMO channels," in *Proc. IEEE Int. Symp. Information Theory*, Seattle, WA, Jul. 2006, pp. 2622–2626.
- [40] B. Banister and J. Zeidler, "Feedback assisted stochastic gradient adaptation of multiantenna transmission," *IEEE Trans. Wireless Commun.*, vol. 4, no. 3, pp. 1121–1135, May 2005.
- [41] N. Jindal, "A feedback reduction technique for MIMO broadcast channels," in *Proc. IEEE Int. Symp. Information Theory*, Seattle, WA, Jul. 2006, pp. 2699–2903.
- [42] D. Gesbert and M. S. Alouini, "Selective multi-user diversity," in *Proc. Int. Symp. Signal Processing and Information Technology*, Darmstadt, Germany, Dec. 2003.
- [43] S. Sanayei and A. Nosratinia, "Opportunistic downlink transmission with limited feedback," *IEEE Trans. Inf. Theory*, submitted for publication.
- [44] T. Marzetta and B. Hochwald, "Fast transfer of channel state information in wireless channels," *IEEE Trans. Signal Process.*, vol. 54, no. 4, pp. 1268–1278, Apr. 2006.
- [45] T. Thomas, K. Baum, and P. Sartori, "Obtaining channel knowledge for closed-loop multi-stream broadband MIMO-OFDM communications using direct channel feedback," in *Proc. IEEE Globecom*, St. Louis, MO, 2005.
- [46] G. Caire, "MIMO downlink joint processing and scheduling: A survey of classical and recent results," in *Proce. Workshop on Information Theory and Its Applications*, San Diego, CA, Jan. 2006.
- [47] J. Choi and R. W. Heath, "Interpolation based transmit beamforming for MIMO-OFDM with limited feedback," *IEEE Trans. Signal Process.*, vol. 53, no. 11, pp. 4125–4135, Nov. 2005.
- [48] N. Khaled, B. Mondal, R. W. Heath, G. Leus, and F. Petre, "Interpolation-based multi-mode precoding for MIMO-OFDM systems with limited feedback," *IEEE Trans. Wireless Commun.*, submitted for publication.
- [49] A. Gupta and S. Nadarajah, *Handbook of Beta Distribution and its Application*. New York: Marcel Dekker., 2004.
- [50] D. Kershaw, "Some extensions of W. Gautschi's inequalities for the gamma function," *Math. Comput.*, vol. 41, no. 164, pp. 607–611, Oct. 1983.
- [51] I. S. Gradshteyn, I. M. Ryzhik, A. Jeffrey, and D. Zwillinger, *Tables of Integrals, Series, and Products*, 6th ed. San Diego, CA: Academic, 2000.

On Space–Time Trellis Codes Achieving Optimal Diversity Multiplexing Tradeoff

Rahul Vaze, *Associate Member, IEEE*, and
B. Sundar Rajan, *Senior Member, IEEE*

Abstract—Multiple antennas can be used for increasing the amount of diversity (diversity gain) or increasing the data rate (the number of degrees of freedom or spatial multiplexing gain) in wireless communication. As quantified by Zheng and Tse, given a multiple-input–multiple-output (MIMO) channel, both gains can, in fact, be simultaneously obtained, but there is a fundamental tradeoff (called the Diversity–Multiplexing Gain (DM-G) tradeoff) between how much of each type of gain, any coding scheme can extract. Space–time codes (STCs) can be employed to make use of these advantages offered by multiple antennas. Space–Time Trellis Codes (STTCs) are known to have better bit error rate performance than Space–Time Block Codes (STBCs), but with a penalty in decoding complexity. Also, for STTCs, the frame length is assumed to be finite and hence zeros are forced towards the end of the frame (called the trailing zeros), inducing rate loss. In this correspondence, we derive an upper bound on the DM-G tradeoff of full-rate STTCs with nonvanishing determinant (NVD). Also, we show that the full-rate STTCs with NVD are optimal under the DM-G tradeoff for any number of transmit and receive antennas, neglecting the rate loss due to trailing zeros. Next, we give an explicit generalized full-rate STTC construction for any number of states of the trellis, which achieves the optimal DM-G tradeoff for any number of transmit and receive antennas, neglecting the rate loss due to trailing zeros.

Index Terms—Diversity–multiplexing tradeoff, multiple-input–multiple-output (MIMO), space–time codes.

I. INTRODUCTION AND PRELIMINARIES

Consider the quasi-static Rayleigh-fading space–time channel with quasi-static interval T , n_t transmit and n_r receive antennas. The $(n_r \times T)$ received matrix Y is given by

$$Y = \theta HX + W \quad (1)$$

where X is the transmitted codeword $(n_t \times T)$ drawn from a space–time code (STC) \mathcal{X} , H the $(n_r \times n_t)$ channel matrix and W the $(n_r \times T)$ noise matrix. The entries of H and W are assumed to be independent and identically distributed (i.i.d.), circularly symmetric complex Gaussian $\mathcal{CN}(0; 1)$ random variables. STCs are classified into two categories, namely: space–time block codes (STBC) and space–time trellis codes (STTC). Henceforth, we assume \mathcal{X} to be always STTC. The entries of X are drawn from a constellation \mathcal{S} whose size scales with signal-to-noise ratio (SNR) with θ chosen to ensure

$$\mathcal{E}(\|\theta X\|_F^2) = T \text{ SNR}.$$

Manuscript received October 5, 2005; revised July 18, 2006. The work was of B. S. Rajan was supported in part by IISc-DRDO program on Advanced Research in Mathematical Engineering and in part by the Council of Scientific and Industrial Research (CSIR, India) under Research Grant (22(0365)/04/EMR-II). This work was done when the first author was with Beceem Communications Pvt. Ltd., Bangalore, India. The material in this correspondence was presented in part at IEEE International Conference on Communications (ICC 2006), Istanbul, Turkey, June 11–15, 2006.

R. Vaze is with the Electrical and Computer Engineering Department, University of Texas, Austin, TX 78712 USA (e-mail: vaze@ece.utexas.edu).

B. S. Rajan is with the Department of Electrical Communication Engineering, Indian Institute of Science, Bangalore-560 012, India (e-mail: bsrajan@ece.iisc.ernet.in).

Communicated by Ø. Ytrehus, Associate Editor for Coding Techniques.

Digital Object Identifier 10.1109/TIT.2006.883613